



January 2019

Extraction And Purification Of Humic Acid From Leonardite As A Graphene Precursor For Lithium Ion Battery Cathodes

Justin James Baker

Follow this and additional works at: <https://commons.und.edu/theses>

Recommended Citation

Baker, Justin James, "Extraction And Purification Of Humic Acid From Leonardite As A Graphene Precursor For Lithium Ion Battery Cathodes" (2019). *Theses and Dissertations*. 2447.
<https://commons.und.edu/theses/2447>

This Thesis is brought to you for free and open access by the Theses, Dissertations, and Senior Projects at UND Scholarly Commons. It has been accepted for inclusion in Theses and Dissertations by an authorized administrator of UND Scholarly Commons. For more information, please contact zeinebyousif@library.und.edu.

EXTRACTION AND PURIFICATION OF HUMIC ACID FROM LEONARDITE AS A
GRAPHENE PRECURSOR FOR LITHIUM ION BATTERY CATHODES

by

Justin James Baker
Bachelor of Science in Chemical Engineering, University of North Dakota, 2018

A Thesis

Submitted to the Graduate Faculty

of the

University of North Dakota

in partial fulfillment of the requirements

for the degree of


Master of Science in Chemical Engineering


Grand Forks, North Dakota


May
2019

© 2019 Justin James Baker

This thesis, submitted by Justin James Baker in partial fulfillment of the requirements for the Degree of Master of Science in Chemical Engineering from the University of North Dakota, has been read by the Faculty Advisory Committee under whom the work has been done and is hereby approved.


Dr. Michael Mann


Dr. Xiaodong Hou


Dr. Gautham Krishnamoorthy

This thesis is being submitted by the appointed advisory committee as having met all of the requirements of the School of Graduate Studies at the University of North Dakota and is hereby approved.


Dean of the School of Graduate Studies


Date

PERMISSION

Title Extraction and Purification of Humic Acid from Leonardite as a
 Graphene Precursor for Lithium Ion Battery Cathodes

Department Chemical Engineering

Degree Master of Science

In presenting this thesis in partial fulfillment of the requirements for a graduate degree from the University of North Dakota, I agree that the library of this University shall make it freely available for inspection. I further agree that permission for extensive copying for scholarly purposes may be granted by the professor who supervised my thesis work or, in his absence, by the Chairperson of the department or the Dean of the School of Graduate Studies. It is understood that any copying or publication or other use of this thesis or part thereof for financial gain shall not be allowed without my written permission. It is also understood that due recognition shall be given to me and to the University of North Dakota in any scholarly use which may be made of any material in my thesis.

Justin James Baker
April 24, 2019

TABLE OF CONTENTS

LIST OF FIGURES	viii
LIST OF TABLES	x
ACKNOWLEDGMENTS	xii
ABSTRACT	xiii
1 INTRODUCTION	1
1.1 Overview	1
1.2 Scope of Research	6
2 REVIEW OF LITERATURE	8
2.1 Humic Acid Extraction.....	8
2.1.1 Aqueous Solvent Extraction	8
2.1.2 Organic Solvent Extraction.....	10
2.2 Humic Acid from Leonardite	14
2.3 Purification of Humic Acid	17
2.4 Production of Graphene from Humic Acid	21
2.5 Applications of Graphene in Lithium-Ion Batteries.....	25
2.5.1 Typical methods of Incorporating Graphene into Lithium-Ion Batteries ..	25
2.5.2 In-Situ Synthesis of Graphene from Humic Acid.....	28
3 EXTRACTION OF HUMIC ACID.....	32
3.1 Introduction	32
3.2 Experimental Procedures.....	33

3.2.1	Optimizing Extraction Parameters/DOE Setup	33
3.2.2	Materials and Methods.....	35
3.2.3	Materials Characterization	35
3.3	Results and Discussion.....	36
3.3.1	Alkaline Extraction	36
3.3.2	Organic Solvent Extraction.....	42
3.3.3	Comparison of Extraction Methods	47
3.4	Conclusion.....	49
4	PURIFICATION OF HUMIC ACID.....	50
4.1	Introduction	50
4.2	Experimental Procedures.....	52
4.2.1	Ash and Silicate Removal.....	52
4.2.2	Removal of Residual Salts	53
4.2.3	Removal of Iron and Other Metallic Impurities	53
4.2.4	Materials Characterization	53
4.3	Discussion.....	53
4.3.1	Ash and Silicate Removal.....	54
4.3.2	Removal of Residual Salts	56
4.3.3	Removal of Iron and Other Metallic Impurities	57
4.4	Conclusion.....	58
5	GRAPHENE-MODIFIED LITHIUM IRON PHOSPHATE SYNTHESIS AND ELECTROCHEMICAL TESTING	59
5.1	Introduction	59
5.2	Experimental Procedures.....	60

5.2.1	LFP/G Synthesis	60
5.2.2	Materials Characterization	61
5.2.3	Electrochemical Testing.....	61
5.3	Results and Discussion.....	62
5.3.1	Crystal Structure Analysis by XRD.....	62
5.3.2	Morphology Analysis by SEM	63
5.3.3	Raman Spectrometry Analysis.....	68
5.3.4	Carbon Content	69
5.3.5	Electrochemical Performance	70
5.4	Conclusions	73
6	FUTURE INSIGHTS.....	75
6.1	Continuation of Research	75
6.1.1	Overview.....	75
6.1.2	Optimization of Graphene-Modified Lithium Iron Phosphate Synthesis Procedure	75
6.1.3	Fractionation of Humic Acid	76
6.2	Potential Applications	77
	REFERENCES	78

LIST OF FIGURES

1.1-1 Idealized Humic Acid and Graphene Oxide Structures.....	5
1.1-2 Proposed Humic Acid Chemical Structure.....	5
2.1.2-1 Three Solvents Which Easily Dissolve Humic Acid when Mixed with Water.....	12
2.1.2-2 Proposed Humic Acid Extraction Process Utilizing Acetone-Water Mixture.	13
2.4-1 Idealized Humic Acid and Graphenol Structures	22
2.4-2 SEM Images of Single Crystalline Graphene Formed from Annealing Humic Acid.....	23
2.5.2-1 Schematic of Graphene-Modified Tin-Oxide Synthesis Process	30
3.3.1-1 Main Effects Plot for Alkaline Extraction DOE with Yield as Sole Response.....	37
3.3.1-2 Main Effects Plot for Alkaline Extraction DOE with Overall Purity as Sole Response	39
3.3.1-3 Main Effects Plot for Alkaline Extraction DOE with Iron Content as Sole Response	40
3.3.2-1 Main Effects Plot for Organic Solvent Extraction with Yield as Sole Response	43
3.3.2-2 Main Effects Plot for Organic Solvent Extraction with Overall Purity as Sole Response	44
3.3.2-3 Main Effects Plot for Organic Solvent Extraction with Iron Content as Sole Response	45

5.3.1-1 XRD Profiles of LFP/G A, LFP/G B, and LFP Reference Samples	62
5.3.1-2 Close-up of (002) Graphitized Carbon Peak Observed in LFP/G A and LFP/G B XRD Profiles.....	63
5.3.2-1 SEM Image of LFP Reference Sample at 100x Magnification	64
5.3.2-2 SEM Image of LFP Reference Sample at 5000x Magnification	64
5.3.2-3 SEM Image of LFP/G A Sample at 100x Magnification	65
5.3.2-4 SEM Image of LFP/G A Sample at 5000x Magnification	66
5.3.2-5 SEM Image of LFP/G A Sample at 20,000x Magnification	66
5.3.2-6 SEM Image of LFP/G B Sample at 100x Magnification.....	67
5.3.2-7 SEM Image of LFP/G B Sample at 5,000x Magnification.....	68
5.3.3-1 Raman Spectra of LFP/G and LFP Reference Samples	69
5.3.5-1 Charge/Discharge vs Voltage Profiles for Coin Cells Prepared with LFP/G and LFP Reference Samples	70
5.3.5-2 Cycling Data for Coin Cells Prepared with LFP/G and LFP Reference Samples	71
5.3.5-3 Rate Performance of Coin Cells Prepared LFP/G and LFP Reference Samples	72

LIST OF TABLES

1.1-1 Popular Lithium-Ion Battery Chemistries and Their Attributes	3
2.1.1-1 Summary of Research Discussed in Section 2.1.1	10
2.1.2-1 Summary of Research Discussed in Section 2.1.2	14
2.2-1 Summary of Research Discussed in Section 2.2	17
2.3-1 Summary of Research Discussed in Section 2.3	20
2.4-1 Summary of Research Discussed in Section 2.4	24
2.5.1-1 Summary of Research Discussed in Section 2.5.1	28
2.5.2-1 Summary of Research Discussed in Section 2.5.2	31
3.2.1-1 Design of Experiment for Humic Acid Alkaline Extraction Conditions.....	34
3.2.1-2 Design of Experiment for Humic Acid Organic Solvent Extraction Conditions ..	35
3.3-1 XRF Elemental Composition of Leonardite Products Source Fines	36
3.3.1-1 Yield, Overall Purity, and Iron Content for Alkaline Extraction DOE	37
3.3.1-2 Alkaline Extraction Optimum Conditions and Ranks per Response.....	40
3.3.1-3 Comparison of Minitab Predictions vs. Lab-Obtained Results from Optimized Alkaline Extraction Procedure	41
3.3.2-1. Yield, Overall Purity, and Iron Content for Organic Solvent Extraction DOE....	42

3.3.2-2 Organic Solvent Extraction Optimum Conditions and Ranks per Response	46
3.3.2-3 Comparison of Minitab Predictions vs. Lab-Obtained Results for Optimized Organic Solvent Extraction Procedure.....	47
3.3.3-1 Comparison of Optimized Conditions and Extraction Results for Alkaline and Organic Solvent Procedures.....	48
4.3.1-1 Silicon and Ash Contents of Filtered and Centrifuged Humic Acid Samples.....	54
4.3.1-2 Silicon and Ash Contents of Humic Acid Before and After Acid Treatment	55
4.3.1-3 Ash Contents of Humic Acid Before and Treatment with Chelating Agent	56
4.3.2-1 Elemental Compositions of Pre-wash and Washed Humic Acid	56
4.3.3-1 Elemental Compositions of Humic Acid Sample Before and After Treatment with Chelating Agent	57
5.3.4-1 Carbon Contents for LFP/G and Reference Samples	69

ACKNOWLEDGEMENTS

I wish to express my sincere appreciation to the members of my advisory committee; Dr. Michael Mann, Dr. Xiaodong Hou, and Dr. Gautham Krishnamoorthy, for their guidance and support during my time in the master's program at the University of North Dakota. I would also like to thank Dr. Yong Hou and the employees and staff at Clean Republic, LLC for their help and collaboration with this research. Other graduate students and personnel I would like to personally thank for their assistance are Justin Mann, Andrew Dockter, Shuai Xu, and Harry Feilen.

ABSTRACT

Lithium ion batteries present a promising solution for energy storage applications which can be utilized to make green energy generation from sources such as wind and solar more practical. Lithium iron phosphate is an attractive battery cathode material due to its long lifespan, safety and stability, and environmentally friendly chemistry. One shortcoming of lithium iron phosphate is its inherently low conductivity, which is commonly overcome through the addition of conductive carbon. Graphene is a two-dimensional nanomaterial comprised of a single layer of carbon atoms, which displays excellent electrical, thermal, and mechanical properties. Commercial incorporation of graphene into battery electrode materials is limited due to the high cost of graphene.

Humic acid is a naturally occurring substance which exhibits properties similar to those of graphene oxide, a common graphene precursor material. High molecular weight humic acid has been proven capable of reducing to graphene that is functionally identical to graphene synthesized from graphene oxide. Humic acid can be found naturally in soils, coals, and other decayed plant matter. North Dakota leonardite, a form of oxidized lignite coal, was used in this research due to its low cost and high humic acid content. This thesis details a study on the feasibility of obtaining a high-purity humic acid material from North Dakota leonardite which can be used as a graphene-precursor in the preparation of lithium-ion battery cathode materials.

Major goals of this research included: i) develop an extraction method to obtain humic acid at acceptable yields while minimizing iron, ash, and other impurities, ii) identify and develop additional purification steps necessary to reduce the level of impurities in the extracted humic acid to acceptable levels for highly technical applications such as lithium-ion battery components, iii) develop a method of synthesizing graphene-modified lithium iron phosphate cathode material using purified humic acid as a graphene precursor, and iv) verify the formation of graphene and increase in electrochemical performance of graphene-modified lithium iron phosphate cathode materials in comparison to reference lithium iron phosphate samples.

To meet these goals and prove or disprove the hypothesis, the research was broken down into five main areas: i) testing and developing an optimized humic acid extraction procedure, ii) testing various processes for reducing impurities in extracted humic acid, iii) testing various methods for synthesizing lithium iron phosphate which were conducive to using humic acid as a carbon source, allowing for adequate mixing and interaction between the humic acid and active material, iv) verifying the formation of graphene through a variety of materials characterization methods, and v) determining the improvement in electrochemical performance of coin cells prepared with graphene-modified lithium iron phosphate compared to reference cells.

The extraction process and purification regime developed in this research has resulted in a procedure for reliably obtaining high-purity humic acid from North Dakota leonardite materials. Ash and iron contents in purified humic acid samples have been less than 0.50% and 0.01%, respectively, on a dry mass basis. Lithium iron phosphate materials have been synthesized using humic acid which exhibit multiple characteristics

of graphene-modification. Coin cells prepared with graphene-modified lithium iron phosphate materials exhibited a reversible specific capacity of 145 mAh/g at a charge/discharge rate of 0.1C, which is an approximately 25% increase when compared to coin cells prepared with reference lithium iron phosphate material. This research has displayed that humic acid is a viable, low-cost alternative to graphene oxide for the synthesis of graphene-modified battery cathode materials.

1 INTRODUCTION

1.1 Overview

Over the recent years, the demand for clean, sustainable energy has grown due to increasing concern over the negative impact that fossil fuels have on the environment. Technologies have advanced yielding cheaper and more practical wind and solar electrical generation, as well as electric vehicles (EVs). Although these technologies have become more prevalent, they still have not had a major impact on the use of fossil fuels for energy production. One of the main roadblocks preventing sustainable energy from replacing fossil fuels is that technologies such as wind and solar cannot provide on-demand power generation, instead generating electricity under optimal conditions such as when the sun is shining or the wind is blowing. This puts renewable energy at a considerable disadvantage when compared to fossil fuels which can be stored and used to match energy generation with demand. For sustainable energy systems and EVs to become more practical, an efficient electrical energy storage system needs to be developed. An ideal electrical storage medium would be cost effective as well as have the following properties: high capacity, high charge/discharge rates, high stability and safety, and environmentally compatible.

Lithium ion batteries (LIBs) are currently most likely to meet these energy storage requirements due to their high energy densities, low weight, and good lifespan [1].

Several varieties of LIBs exist, each with unique properties that make them suitable for

different application. Table 1.1-1 list several popular lithium ion cathode chemistries as well as their strengths, benefits, and typical applications.

Several battery chemistries could potentially be used for large-scale energy storage based on Table 1.1-1. Lithium Nickel Manganese Cobalt Oxide (NMC) cathode material boasts excellent capacity and good power, safety, cycle life, and price. However, NMC relies on cobalt and nickel metals, both of which can result in damage to the environment through current mining practices. Lithium Nickel Cobalt Aluminum Oxide cathodes exhibit similar characteristics to NMC, but again relies on cobalt and nickel, and suffers from lower safety, and higher costs. LIBs prepared with lithium iron phosphate (LFP) cathodes are of particular interest due to their intrinsic stability, long lifespan, and low environmental impact. One downside to LIBs that utilize LFP as the cathode material is low specific capacity due to the inherently low conductivity of the active material. This can be overcome by adding carbon to the active material, often in the form of graphite, carbon black, or simple sugars [2]. A side effect of this is a decrease in density of the active material, thus resulting in a lower energy density. One solution to this is to use graphene-like materials to coat the active cathode material. Graphene's high surface area and excellent ion mobility have been shown to improve several properties of LIB cathode materials such as energy density, cycling stability, and rate capability [3].

One obstacle to using graphene in LFP cathodes is incorporating the graphene into the active material on the nano-scale. Graphene-wrapped, nano-sized LFP particles

Table 1.1-1 Popular Lithium-Ion Battery Chemistries and Their Attributes.

Cathode Material	Manufacturers	Typical Applications	Date Commercialized	Specific Capacity	Specific Power	Safety	Cycle Life	Price	Comments
Lithium Nickel Manganese Cobalt Oxide ("NMC", $\text{LiNi}_x\text{Mn}_y\text{Co}_z\text{O}_2$)	Imara Corporation, LG Chem, Nissan Motor	EV's, medical devices, industrial, E-bikes	2008	****	***	***	***	***	High specific capacity and power, good safety and cost. Still relies on cobalt.
Lithium Manganese Oxide ("LMO", LiMn_2O_4)	E-One Moli Energy, Hitachi, Samsung	Power tools, medical devices, EV's	1996	***	***	***	**	***	High power, safer than LCO, but low capacity. Often mixed with NMC
Lithium Iron Phosphate ("LFP", LiFePO_4)	Phostech Lithium Inc, Simpliphi Power	Segway, power tools, energy storage	1996	**	****	****	****	***	High power, excellent stability and lifespan, but low specific capacity. One of safest Li-ions.
Lithium Cobalt Oxide ("LCO", LiCO_2)	Sony, E-One Moli Energy	Mobile phones, tablets, laptops	1991	****	**	**	**	***	High specific capacity, but low power and safety. High cost.
Lithium Nickel Cobalt Aluminum Oxide ("NCA", LiNiCoAlO_2)	Panasonic, Saft Groupe S.A.	EV's, medical devices, industrial	1999	****	***	**	***	**	High specific capacity, good power and lifespan. Poor price and safety.

have been achieved through the mixing of reduced graphene oxide (rGO) with LFP materials [4]. These particles exhibited excellent capacity at high discharge rates, and low rate capacity decay even at charge/discharge rates up to 20C. A graphene-modified LFP composite was synthesized by mixing graphene oxide (GO) in an oil-water emulsion with LFP precursor solutions [5]. After thermal treatment, cells were prepared with this composite that were able to achieve a capacity of 160 mAh/g at 0.1C charge/discharge rate. While these methods were successful in producing graphene-modified LFP, they rely on graphene oxide based materials which can have high costs. The high material cost is the main barrier to the commercial use of graphene in lithium-ion batteries. A solution to this problem is to find a material which is inexpensive and can be used to form graphene or graphene-like carbon.

A potential low-cost alternative to conventional graphene precursors is humic acid. Humic acid (HA) is a polymer-like component of soil and decayed organic matter which is generally considered as the fraction of soil which is soluble in basic conditions, and insoluble at neutral and acidic pH levels. The organic fraction of soil which is soluble throughout the entire pH range are fulvic acids (FA), which are similar to HAs, but much lower in molecular weight. There is no defined molecular structure for HAs, instead they exist as a wide range of molecular weights with various combinations of carboxyl and hydroxyl groups. Figure 1.1-1 compares an idealized HA structure with a graphene oxide molecule [6]. Both structures share a carbon lattice core with a high degree of edge oxidation in the form of carboxyl, carbonyl, and hydroxyl functional groups. Figure 1.1-2 details a more complex HA model based on extensive testing and analysis [7]. This

proposed HA structure depicts alkane chains of various lengths linking central aromatic carbons, with a high degree of oxidation and edge functionalization.

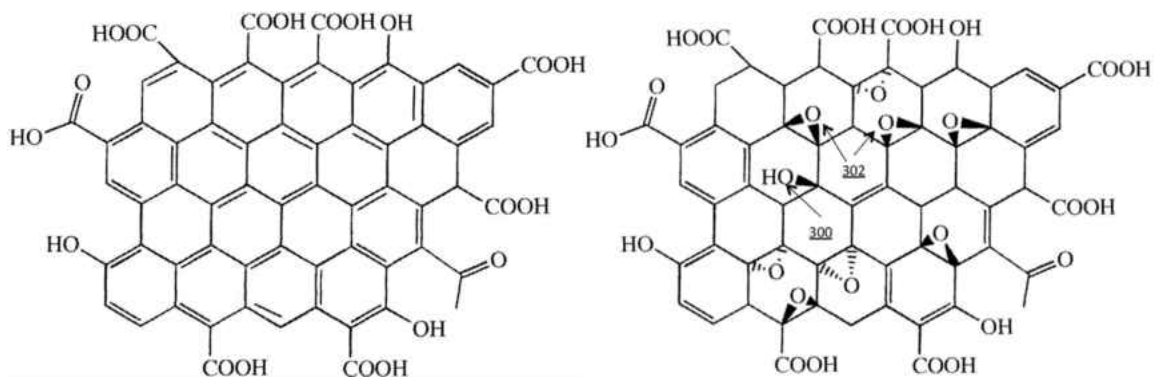


Figure 1.1-1 Idealized Humic Acid (left) and Graphene Oxide Structures (right). Both exhibit a high degree of oxidation with numerous carboxyl and hydroxyl groups. Image credit to G. Beall [6].

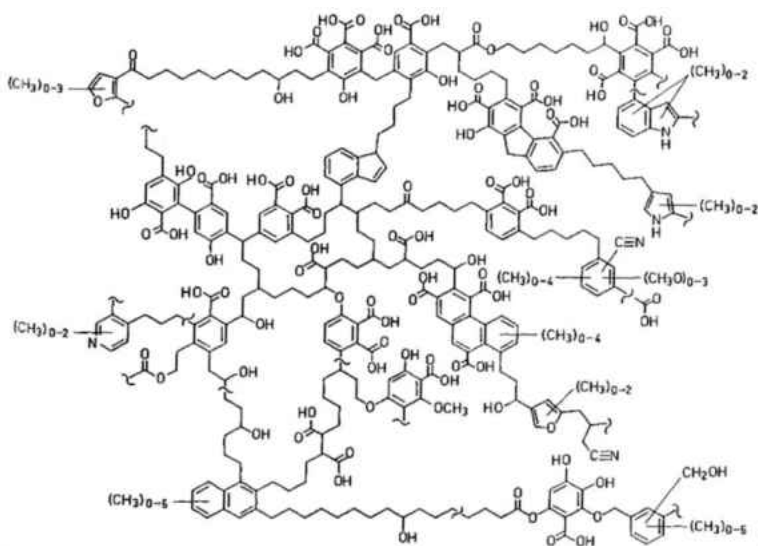


Figure 1.1-2 Proposed Humic Acid Chemical Structure. Carbon chains link various aromatic carbons with a high degree of functionalization. Image credit to H. Schulten and M. Schnitzer [7].

Much work has been done in the area of extracting HA from soils, coal, and other organic matter. The most common methods of extraction involve the use of aqueous

solutions containing strong hydroxide bases, though other organic solvents have been proven to yield similar results. HA produced by a single extraction step often lacks the purity required for technical applications, so further purification is often required. Ash is typically removed by treating the HA with mineral acids. Metallic impurities are often in the form of organic-metallic complexes, and they require the use of strongly oxidizing acids or chelating agents remove them.

Leonardite was used as the starting material from which the HA was extracted for this research. Leonardite is a form of young, oxidized lignite coal which is high in HAs. North Dakota leonardite in particular can contain up to 86% HA on a dry basis [8]. Currently, leonardite is mainly used in non-technical applications, primarily as a fertilizer and soil supplement. In some coal mining operations, leonardite is considered a waste material, meaning that it can be obtained at low cost. There is also an economic aspect in being able to produce a low-cost, highly technical product such as graphene from a low-value raw material such as leonardite.

1.2 Scope of Research

The purpose of this research is to synthesize graphene-modified lithium ion battery cathodes prepared using HA. LFP cathodes will be prepared using HA in order to form graphene-modified lithium iron phosphate (LFP/G). The LFP material will be synthesized by a process which allows for molecular level mixing, and precise particle size control. A key challenge in this work is obtaining sufficient quantities of HA that contains a minimal amount of ash, elemental iron, and other impurities which are detrimental to lithium ion electrode chemistries. The next obstacle is to in-situ produce graphene from HA in the process of LFP synthesis to allow for a homogenous LFP/G

composite and excellent electrochemical performance. Lastly, the process for reducing and converting the HA into graphene and few-layer graphite will have to be developed and optimized to obtain suitable performance in electrochemical testing.

2 REVIEW OF LITERATURE

2.1 Humic Acid Extraction

The topic of extracting HA has seen a great deal of work. A variety of starting materials including soil, coal, and decayed plant matter have been successfully used to obtain HA. Extractions are typically performed one of two ways. The first is the use of a basic solution to dissolve humic and fulvic materials, enabling their separation from insoluble components. The alkaline solution is then acidified to precipitate HA which can then be collected. Solvent extraction is the other method typically used to obtain HA from a precursor material. With careful solvent selection, HA of similar quality and quantity to that extracted by base-acid can be obtained.

2.1.1 Aqueous Solvent Extraction

Aqueous extraction of HA using basic and acidic solutions is the most popular method used today due to its simplicity. The first comprehensive studies on HA were assembled and published by Sprengel in 1826, in which he used alkaline and acidic solutions to extract HA from soil [9]. His method of extraction was similar to the limited work on HA conducted previously, and has been used since due to its ease and effectiveness. This HA extraction procedure utilizing basic and acidic solutions laid the groundwork for what would eventually become the standardized procedure of the International Humic Substance Society (IHSS) for the extraction and quantification of humic and fulvic substances.

In 1959 Frost, Hoepfner, and Fowkes published their findings on extraction procedures for coal and leonardite for obtaining low-ash HA [10]. Their work included using several alkalis to extract lignite slack material as well as leonardite, naturally occurring form of oxidized lignite coal. They found strong evidence that metal ions complexed with HA could be removed by treatment with dilute acid. Washing the extracted HA with water then resulted in a reduced ash content, as low as 0.20% by mass. They also reported that yields of up to 86% percent were possible with this procedure. The work of Frost, Hoepfner, and Fowkes resulted in the first unofficial, but widely accepted procedure for the extraction of low-ash HA by alkaline extraction. Their procedure was followed by many until the IHSS standardized HA extraction procedure was published.

The first standardized procedure was published in 1981 as a handout for members of the International Humic Substance Society (IHSS) [11]. This publication provided guidelines on testing soils and coal for HA with a procedure very similar to that developed by Frost, Hoepfner, and Fowkes. It detailed using 0.1 N NaOH in an amount equal to 10 ml per 1 gram of soil to extract humic materials. This was to be followed by acidification to a pH of 1 using 6 N HCl, and the solids removed from solution by centrifuging or filtration. The resulting raw HA obtained by this procedure is suitable for qualitative analysis or further purification and refinement. This standardized procedure is still used today as the main method for the extraction and quantification of humic and fulvic materials.

Several other procedures have been developed, but still none are as popular or as widely used as the IHSS method. A method similar to the IHSS procedure, but which

utilizes the carbon content of the soil to determine solvent volume was developed by researchers at Nagoya University in 1992 [12]. This procedure, termed the “NAGOYA method”, did not produce HA that was significantly different than HA obtained by the IHSS procedure. It also required users to know the exact carbon content of their soil, which was considered a downside. What can be concluded from all of these works is that the alkaline-based extraction procedure for HA originally developed in 1826 and standardized into the IHSS procedure has proven to be a robust, effective method for obtaining usable quantities of HA from soils and decayed organic matter, and is still being utilized today. Table 2.1.1-1 found below provides a brief summary of the publications discussed in this section.

Table 2.1.1-1 Summary of Research Discussed in Section 2.1.1.

Authors	Year	Notes
C. Sprengel [9]	1826	First publication on extraction of HA using basic and acidic solutions.
C. Frost, J. Hoepfner, W. Fowkes [10]	1959	Obtained high yields of low-ash HA from various coals. Their extraction procedure was widely used until 1981.
International Humic Substance Society [11]	1981	Published first standardized extraction procedures for obtaining HA with a basic solution.
S. Kuwatsuka, A. Watanabe, K. Itoh, S. Arai [12]	1992	Developed HA extraction alternate to IHSS method. Requires exact carbon content of soil, no advantage over IHSS standard.

2.1.2 Organic Solvent Extraction

Aqueous extraction of humic acid has been well-established, and is accomplished with relative ease, but it does have several drawbacks. These include the use of strong acids and bases as well as the requirement for fresh acids and bases for each extraction. Aqueous extraction also requires materials which can handle both high and low pH conditions, which may be a disadvantage when considering the extraction of HAs at large

scale due to high material costs. Both of these challenges have driven researchers to find a suitable organic solvent for the effective extraction of HA from coals and soils.

One of the earliest accounts of the use of an organic solvent used to extract HA is a publication by Thiessen and Engelder in 1930. They extracted HAs from dried decayed wood using hot acetone [13]. The goal of their study was to avoid altering the natural resins, lignins, and organic acids in found in organic materials, as it was believed that strong alkali solutions could damage these compounds. They successfully extracted HAs in quantities sufficient for analysis, indicating that organic solvents such as acetone could be used for efficient extraction.

In search of the perfect solvent for the extraction of HA from coal, Polansky and Kinney performed an exhaustive test of multiple extract solvents in 1947 [14]. Solvent activity was determined by the intensity and how quickly the red-brown color of dissolved HA was observed in treated coal mixed with solvent. Over 250 solvents and solvent mixtures were determined to extract HA with a high yield. It was also found that as carbon chain length increased for linear solvent molecules, the solvent activity rapidly decreased. The solvent they recommended for commercial extraction of HA was a mixture of 50% to 90% acetone and water. Figure 2.1.2-1 depicts three solvents that extracted the highest amounts of HA when mixed with water. Frost, Hoepfner, and Fowkes reported similar findings, detailing that HA could be fully soluble in a 3:1 acetone-water mixture. They also found that high concentrations of calcium ions would facilitate the precipitation of HA from the solvent, so a small amount of mineral acid was needed in the extracting solution [10]. Prolonged contact between the solvent and the original leonardite would dissolve less than 3% of the original leonardite material,

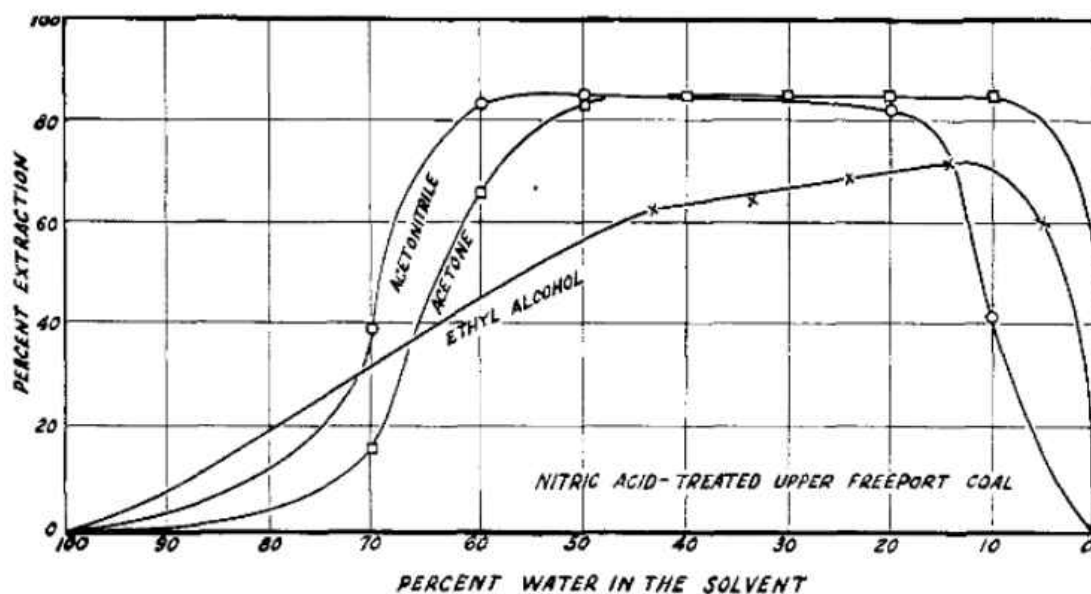


Figure 2.1.2-1 Three Solvents Which Easily Dissolve Humic Acid when Mixed with Water. Image credit to T. Polansky and C. Kinney [14].

indicating that the extraction duration had little effect on the extracted HA. Both of these studies indicate that water-acetone mixtures were well suited for extraction due to their ability to readily and completely dissolve HA.

In 1963, in search of an economic process for the production of HA, Youngs and Frost explored several different methods for the production of low-ash HA from leonardite [15]. The alkaline extraction procedure was not tested due to the requirements for large quantities of acid and base. They reported that an extracting solution of acetone, water, and HCl was most suited to a commercial process as the solvent could be evaporated, recovered, and re-used. The composition of the solvent that was found to work best was 80% acetone and 20% water by volume, along with 10 grams of HCl per 100 grams of leonardite. The purpose of the HCl in the solution is to replace calcium ions in the leonardite with hydrogen in order to reduce ash in the extracted HA. They were

able to obtain a HA product with an ash content of only 1.8% on a moisture-free basis with this procedure. A schematic of their proposed process is depicted in Figure 2.1.2-2. Their conclusions indicated that an organic solvent extraction process would be most economical at production scale compared to floatation and float-sink method.

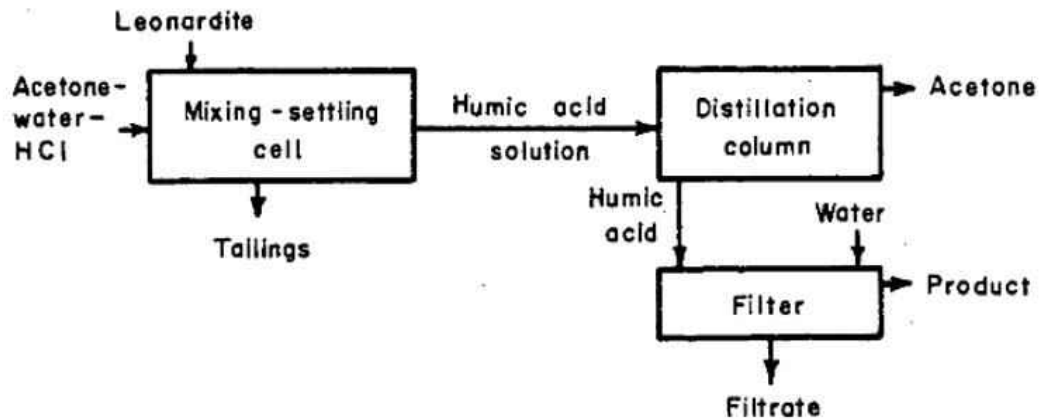


Figure 2.1.2-2 Proposed Humic Acid Extraction Process Utilizing Acetone-Water Mixture. Image credit to R. Youngs and C. Frost [15].

Several other studies have included testing of other organic solvents and solutions. Hayes et al. in 1975 tested multiple solvents including EDA, pyridine, sulpholane, DMF, and EDTA, although none performed as well as the NaOH in the IHSS extraction method [16]. In 1988, Piccolo tested various solvents including DMF and DMSO which resulted in HA of higher purity but much lower yield than that extracted by alkaline procedure [17]. HA obtained using organic solvents was also found to be more aliphatic than those extracted by the IHSS method. Ricca et al. studied the effect of methylation on the solubility of HA in various organic solvents in 2000 [18]. Methylated samples exhibited excellent solubility in CHCl_3 and CH_2Cl_2 , allowing for more advanced analysis and characterization techniques. These publications display that specialized

organic solvents are likely not suitable for efficient extraction of humic materials, but they have more niche applications including fractional extraction, modification of HA, selective modification, and characterization and analysis.

Various research examples have shown that organic solvents are a possible alternative to basic/acidic extractions for obtaining HA. While there is no standardized procedure like the IHSS method for alkaline extraction, most of the research indicates that a solution of 75-80% acetone and 20-25% water, along with a small amount of acid is capable of extracting large amounts of low-ash HA from various sources. Table 2.1.2-1 provides a short summary of the research covered in this section.

Table 2.1.2-1 Summary of Research Discussed in Section 2.1.2.

Authors	Year	Notes
G. Thiessen, C. J. Engelder [13]	1930	First to publish extraction of HA with an organic solvent. Goal was to avoid damaging natural resins, lignins, and organic acids with strong bases.
T. Polansky, C. Kinney [14]	1947	Extensively studied pure organic solvents, binary, and tertiary mixtures for HA extraction. Found acetone-water solutions worked well.
C. Frost, J. Hoepfner, W. Fowkes [10]	1959	Found a 3:1 acetone:water mixture worked well for HA extraction. Needed acid to prevent HA precipitation due to calcium ions.
R. Youngs, C. Frost [15]	1963	Found a water/acetone system worked best for bulk HA extraction. Obtained HA product with 1.8% ash by this procedure.

2.2 Humic Acid from Leonardite

Humic acid is naturally occurring and can be found in plants, decayed organic matter, and most commonly soil. Soils typically have the highest HA content, which can further vary with soil type and location. Coals have been successfully used to obtain HA, as they contain a high percentage of carbon originating from organic matter. Leonardite is

a carbon-rich soil which closely resembles oxidized lignite. Leonardite typically has a high concentration of HA, and North Dakota leonardite is of particular interest due to the fact that it can be comprised of up to 86% HA on a dry, ash-free basis [8].

An early study exhibiting the high HA and FA content for various coals was conducted by Friedman and Kinney in 1950 where alkali-soluble organic acids were extracted from air-oxidized coal [19]. Coal grades tested ranged from lignite to anthracite, with a low-volatile coal yielding the highest amounts of HA at over 95% by mass, lignite at 73%, and anthracite only 7%. This study exhibited that oxidized coals may be suitable feedstocks for the production of HA, and that lower-rank coals may be superior to higher-ranked coals, although there was no direct correlation between coal rank and yield of HA.

One of the first studies testing North Dakota leonardite for HA production was by Frost, Hoepfner, and Fowkes in 1959, in which they compared the leonardite to lignite coals [10]. Multiple extract solutions were tested, and it was determined that leonardite was a suitable candidate for bulk HA production, containing up to 86% HA by mass with low ash contents. Extraction of untreated lignite coal yielded only 5% HA by mass, a fraction of what was attained by leonardite. This exhibits that leonardite is a suitable source of HA as it can contain up to 86% HA by mass and requires no pretreating steps, unlike coals.

In 1963, Youngs and Frost studied several methods for the extraction of HA from leonardite [15]. Leonardite was selected due to the high HA content. Alternatives to the typical alkali extraction process were considered due to the high acid and base requirements of the alkaline method. They were able to obtain extract yields of HA

around 65% with a 1.8% ash content using a water-acetone extraction method. This study implicated the potential for large-scale production of HA using an organic solvent extraction and leonardite as a raw material.

The suitability of leonardite as a source of HA was again proven by Beall in 2013 when he patented a method for the production of graphene and functionalized graphene [6]. The patented process essentially converts purified HA into a material termed as “graphenol”, which can be easily reduced to graphene-like sheets. North Dakota leonardite was specifically mentioned due to its high HA content, making it a favorable source for this application. Several other publications specify leonardite as a source used to obtain HA for technical applications. Leonardite-derived HA was used to synthesize single-crystal graphene on a copper substrate in 2014 for comparison to graphene synthesized from graphene oxide (GO) [20]. Reduced HA from leonardite, in 2015, was used as a nano-filler in polyurethane composite materials to increase strength and other mechanical properties [21]. In 2018, leonardite-derived HA was used to synthesize graphene-SnO₂ composite and increase the conductivity and mechanical resilience of the electrodes for LIB usage [3]. These are only a few examples of the highly technical applications for which HA obtained from leonardite has been utilized.

While multiple potential sources for obtaining HA exist, North Dakota leonardite is of particular interest due to its high HA content of approximately 86% on a dry, ash-free basis. Other sources of HA such as soils and decayed plant matter suffer from low HA yields or require oxidizing pretreatments as is the case for many coals. Leonardite has been shown to be suitable with both alkaline and organic solvent extraction techniques, and is capable of yielding HA suitable highly technical applications such as

in battery electrode materials and graphene formation. Table 2.2-1 provides a short summary of the major research covered in this section.

Table 2.2-1 Summary of Research Discussed in Section 2.2.

Authors	Year	Notes
L. Friedman, C. Kinney [19]	1950	Obtained high amounts of HA from air-oxidized coals. Lower-grade coals tended to yield more HA.
C. Frost, J. Hoeppepner, W. Fowkes [10]	1959	First to use North Dakota leonardite as source of HA. Obtained very high yields of HA, up to 86% by mass using alkaline extraction.
R. Youngs, C. Frost [15]	1963	Used leonardite to test feasibility of production-scale HA extraction by organic solvent extraction. Achieved HA yields around 65% with 1.8% ash.
G. Beall [6]	2013	Patented process for producing graphene from HA via "graphenol" intermediate. Used leonardite due to high HA content and low ash.

2.3 Purification of Humic Acid

Direct extraction of humic acid rarely results in a product with a suitable level of impurities for most technical applications. Ash is the most typical impurity, comprised mostly of silicates which can be removed through the use of mineral acids or other treatments. Specific applications using HA also require minimal amounts of metallic impurities as well. For battery applications, iron needs to be minimized to prevent electrode poisoning and short circuits. Metals are often removed with acids or chelating agents. Other more novel approaches to purifying HA have been attempted with varying degrees of success.

In an attempt to reduce ash content, Frost, Hoeppepner, and Fowkes used hydrochloric acid to treat their extracted HA [10]. The HA was treated with hot, 5M HCl followed by cold concentrated HCl. The result was a reduction in ash from 1.0% to 0.2%. Ultimate analysis comparing the untreated and treated HA indicates that the purification

step had significant impact on the composition of the HA, as after acid treatment, carbon content decreased while oxygen content increased. This work displays that impurities in HA can be reduced by a simple water washing step or with a light acid treatment. HA with very low ash contents can be obtained by treatment with strong acids, although they have can substantially change the composition of the HA.

In a section on the purification of HA in *Humus Chemistry* by Stevenson, several methods for reducing ash and impurities in HA are reviewed [22]. Several impurities listed commonly found in HA include salts, oxides, silicates, and clays. Repeated precipitation with dilute acid, as well as the use of an ion-exchange resin are both suggestions on how to reduce ash content. Acid solutions containing hydrofluoric acid (HF) are also mentioned as being successful at reducing ash content, but they are mentioned as having the ability to chemically modify the HA and increase difficulty with characterization. Another mechanism proposed by the author for the removal of ash is due to the complete removal of FA, which may have strong metal linkages. The information provided by this publication provides understanding as to where ash and impurities in HA originate as well as several methods on how to remove them.

Further study on the effects of acid mixtures for HA purification was conducted by Piccolo in 1988 [17]. A 0.50% HCl-HF mixture was used to treat HA and reduce impurities. The purification step significantly reduced the ash content of the HA in all samples, though a loss of organic matter was also observed. An increase in carboxyl groups as well as changes in the molecular sizes of the HA were also attributed to the acid treatment, and thought to be due to a condensation-type reaction mechanism. The work presented in this article establishes guidelines for the chemical removal of ash from

HA via HF-HCl mixture, as well as offers an explanation to the observed changed in size of the HA molecules.

The influence of pH on the solubility of HA-metal complexes was studied by Garcia-Mina in 2006 [23]. It was found that as pH increases, the solubility of metal complexes generally increased. This was found to be especially true for copper and iron HA complexes. The extent and degree of which the HA is complexed also has a significant effect on solubility. At the same conditions, FA-metal complexes presented higher solubility than HA complexes. This publication aided in increasing the understanding of the governing factors of metal-HA solubility and the characteristics of these complexes.

There are several other publications which have aided in the understanding of impurities present in HA. Ion-exchange resins have been used to reduce metal cations which were bound to HA, resulting in a final ash content of 1.6% [24], which is still relatively high. Ion exchange may be best utilized as part of a process after the bulk of impurities have been removed. Floatation and float-sink processes used to clean coal have also been used to reduce the ash content of HA [15]. In their testing, Frost and Youngs were able to obtain a high yield of HA with a moderate ash content by the float-sink process, but ultimately ruled both methods unsuitable for HA production using leonardite. Information regarding the formation and removal of metal cations complexed with HA was reviewed in a section of *Methods of Soil Analysis: Part 3-Chemical Methods* [25]. It was also suggested that certain chelating agents may reduce total ash content by weakening bonds between HA and clays. Specific guidelines and procedures for chelating agent use and metal-ion reduction were published by Flaschka in 1959 [26].

The information published was not specified for use in purifying humic substances, but has proven to be quite capable of reducing impurities in HA. These works have all aided in the understanding of the interactions between metal ions, ash, and HA and have proven useful to developing a purification procedure to reduce impurities in HA to acceptable levels.

There are multiple methods that may be useful for reducing various impurities which can be present in HA. Ash as a component can in most cases be removed through adequate extraction techniques, and residual ash reduced through treatment a weak HF-acid mixture or water. In order to remove metals in cation form, chelating agents which form strong bonds with metal ions may be used to break metal-HA complexes. Ion exchange resins have also been used to reduce metallic impurities, but they need to be coupled with another impurity-reduction method to be effective. All of these methods can be utilized to obtain low-impurity HA, although some are more effective than others.

Table 2.3-1 provides a summary of the main publications covered in this section as well as the impurities targeted by the research.

Table 2.3-1 Summary of Research Discussed in Section 2.3.

Authors	Year	Notes	Target Impurities
H. A. Flaschka [26]	1959	Published guidelines and procedures for using chelating agents to remove metal ions from solution.	Complexed metal ions
C. Frost, J. Hoeppepner, W. Fowkes [10]	1959	Reduced ash content in HA samples using acid and water wash steps. Observed changes in HA composition when treated with strong acid.	Ash
F. J. Stevenson [22]	1982	Published extensive information on ash and impurities found in HA as well as techniques for their removal.	Ash, complexed metal ions, salts
A. Piccolo [17]	1988	Established guidelines for HCl-HF use to reduce ash in HA. Proposed condensation-type reaction as reason for increase in observed molecular size.	Ash
J. M. Garcia-Mina [23]	2006	Linked HA-metal complex solubility with pH. Zinc, iron and copper identified as forming most stable complexes.	Complexed metal ions

2.4 Production of Graphene from Humic Acid

Graphene is a material of significant interest due to its excellent thermal, electrical, and mechanical properties, among others. It was discovered in 2004 and obtained by the mechanical exfoliation of graphite [27]. There exists a variety of methods for the production and synthesis of graphene that have their own unique attributes and drawbacks. The most popular methods of graphene synthesis for general use is by the reduction of GO. Graphene precursors can be quite costly however, so an alternate material for graphene production is desirable. One substance that shares many of the traits of GO is HA. HA can have a high molecular weight with a lattice-like structure and a high degree of oxidation [7]. Graphene-like materials synthesized from typical precursors, in some applications, may be inferior to materials synthesized from HA due to the natural porous structure the HA can induce in graphene [28, 29]. The following research will show that HA is capable of producing graphene under the right conditions.

One of the earlier publications linking HA and the graphene was a patent by Beall in 2013 in which he details a novel process for graphene production from HA via a “graphenol” intermediate [6]. This graphenol is formed by reacting HA with hydrogen over a catalyst, reducing HA and the forming of abundant hydroxyl groups. A comparison between an idealized HA molecule and an idealized graphenol molecule is depicted in Figure 2.4-1. These graphenol molecules reportedly have extremely high molecular weights and upon thermal treatment, form products with a high degree of similarity to graphene. Beall’s patent established that HA is capable of forming graphene, albeit with a few intermediate steps.

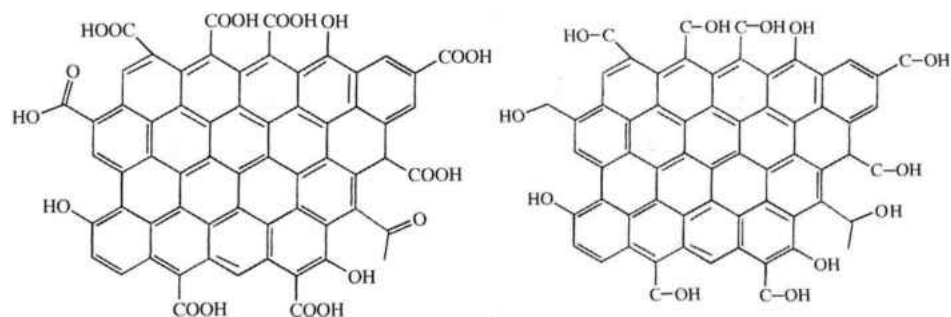


Figure 2.4-1 Idealized Humic Acid (left) and Graphenol (right) Structures. Image credit to G. Beall [6].

In 2014, Beall et al. investigated and compared the formation of graphene from several sources including HA [20]. All carbon sources were found to produce a thin graphite layer on a copper substrate when carbonized at a temperature of 1050 °C, but only the leonardite-derived HA was able to form single graphene crystals upon annealing at 1100 °C. Figure 2.4-2 displays SEM images of single crystalline graphene formed from annealing HA. Raman spectrum analysis confirmed the formation of graphene from all three carbon sources, but graphene synthesized from HA exhibited the fewest layers and smallest number of defects. This research displayed that pure HA is capable of producing crystalline graphene with a high level of purity without needing an intermediate synthesis step.

To gain further understanding of graphene produced from HA, Beall and Powell in 2015 directly compared HA and GO as graphene precursors [30]. The precursors were determined to be similar in size, sheet thickness, and oxygen content. Various reducing methods were used to form graphene-like carbon, and samples prepared using HA typically exhibited higher carbon contents and lower I^D/I^G ratios. This means that the HA-based graphene had fewer defects than graphene which was synthesized from GO.

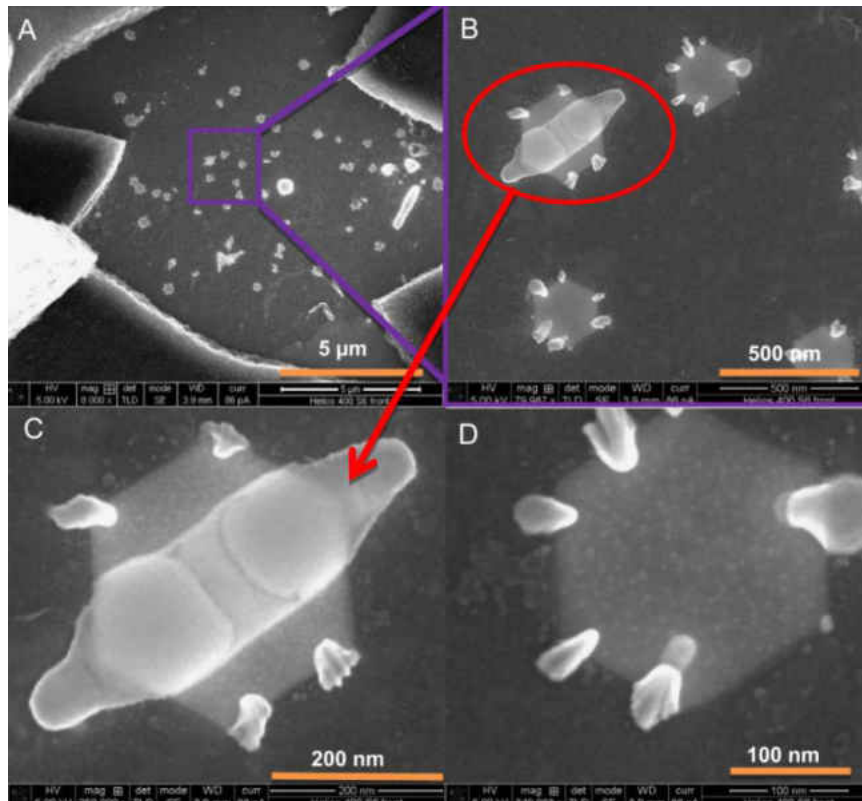


Figure 2.4-2 SEM Images of Single Crystalline Graphene Formed from Annealing Humic Acid. Image credit to Beall et al. [20].

This study proved that not only was HA suitable for graphene formation, but that it actually produced a higher quality graphene product than more popular precursors such as GO. Similar results were reflected in research by Baskakov et al. [31], and Beall and Duraia [32]

Electrochemical properties of graphene synthesized from HA materials were tested in 2018 by Si et al. where Li-ion anodes were prepared with carbonized HA [33]. The effect of carbonization temperature on electrode performance was tested for HA heated between 2200 and 2800 °C. Samples carbonized at higher temperatures exhibited finer crystal structure, higher specific capacity, and better high-rate performance than those prepared at lower temperatures. All samples prepared using reduced HA performed

better than those prepared using graphite, a common material used in LIB anodes. The findings of this research indicate that graphene prepared from HA performs better as a LIB anode material as carbonization temperature increases.

Due to its excellent properties and characteristics, graphene is a highly desired material for a wide variety of applications. HA has been proven to produce graphene that is functionally identical to graphene produced by more popular precursors. In some instances, HA produced graphene of higher quality than that which was synthesized from GO, and has proven to be a suitable material for LIB anodes and for producing graphene-modified cathode composites [3]. The conditions under which graphene is synthesized have also been shown to have a significant impact on electrochemical performance, with better results obtained at higher carbonization temperatures. Table 2.4-1 summarizes the main research covered in this section. Based on this research, it can be concluded that HA is a suitable carbon source for the formation of graphene, and based on its similarities to GO, may be used as a direct substitute for GO in established graphene synthesis procedures.

Table 2.4-1 Summary of Research Discussed in Section 2.4.

Authors	Year	Notes
G. Beall [6]	2013	Patented process for graphene formation from leonardite-derived HA via graphenol intermediate.
G. Beall, E. M. Duraia, Q. Yu, Z. Liu [20]	2014	Tested several graphene precursors including HA and graphenol. Exhibited that pure HA was capable of forming graphene without intermediate step.
G. Beall, C. Powell [30]	2015	Compared HA to GO as a graphene precursor. Graphene from both precursors was functionally identical.
D. Si, G. Huang, C. Zhang, B. Xing, Z. Chen, L. Chen, H. Zhang [33]	2018	Found strong link between increase in carbonization temperature and enhanced electrochemical performance of graphene anode materials prepared from HA.

2.5 Applications of Graphene in Lithium-Ion Batteries

Lithium-ion battery technology is a source of high-energy, lightweight power that has yet to be rivaled in terms of performance. In order to improve the electrical properties of LIBs, carbon is often added to the electrode materials. LFP electrodes in particular benefit from added carbon to overcome inherently low conductivity in the active material. Carbon is typically added from sources such as sugars, graphite, or carbon black [1, 34]. Graphene is also a desirable material due to its electrical and mechanical properties, and it is seeing increased use and applications in LIB technology.

2.5.1 Typical methods of Incorporating Graphene into Lithium-Ion Batteries

One of the challenges of incorporating graphene into various Li-ion electrode chemistries is ensuring an adequate and even mixture that will result in a uniform carbon coating that will perform as desired. Obtaining satisfactory results through the direct mixing of active materials with graphene is often unsatisfactory as the graphene flakes will form agglomerates and the resulting mixture will be lacking the intimate contact between the active material and carbon source required for enhanced performance [4, 35]. Other synthesis methods typically entail growing active material on graphene sheets, or growing graphene in-situ on the active material [36]. Due to the wide range of Li-ion chemistries and that LFP cathodes benefit significantly from carbon coating, the main focus of the following articles will be on the implementation of graphene into LFP active materials to form LFP/G.

One of the earliest publications detailing the formation of LFP/G was by Zhou et al. in 2011 in which LFP precursors were mixed with GO nanosheets that were reduced

to graphene during calcination [4]. GO was added to LFP synthesized via sol-gel method, which resulted in LFP/G material with a capacity of almost 150 mAh/g at 0.1C. Samples prepared using both glucose and GO exhibited the highest capacity and best high-rate performance, indicating that the GO nanosheets may not be making adequate contact with LFP particles, and the supplemental carbon was enhancing the contact between graphene and LFP. It was also theorized that folding and distortion of the GO sheets was possible due to the drying procedure used, which may have had an effect on electrochemical performance. This publication displayed the enhanced performance of LFP/G as well as the importance of the methods used to incorporate graphene into the active material. Similar findings were reported by Yang et al. in 2012 [37], Zhang et al. in 2012 [38], Dhindsa et al. [39], Liu et al. in 2014 [40], and Tao et al. in 2014 [41].

An application where graphene was directly applied as a conductive coating for LFP was presented by Su et al. in 2012 [42]. Graphene prepared from graphite was added to LFP precursors and sintered to form LFP/G. The LFP/G sample exhibited a rather low specific capacity of 140 mAh/g which rapidly declined. This was attributed to poor interaction between the graphene and LFP particles via a “dot on plane” mode of contact. They found that samples prepared with graphene sheets as well as a source of amorphous carbon had a much higher capacity due to the enhanced interaction between the LFP particles and the graphene. This research again stressed the importance of the mixing method used to incorporate graphene into LFP and suggests that pure graphene itself may not be a good material for enhancing the conductivity of the active material. Similar findings were reported by Wen et al. in 2018, where graphene was mixed with active LFP

material and binding agents to prepare LFP cathodes [43]. The poor interaction between graphene and LFP particles resulted in performance that was less than desired.

There are several other examples of research where LFP/G was synthesized by more novel approaches. In 2014 Mo et al. synthesized LFP/G using GO in a water-oil emulsion, based on the concept of space confinement and allowing for precise particle size control [5]. Their LFP/G composites exhibited capacities of 160 mAh/g at 0.1C, and over 80 mAh/g at a 60C rate. Electrophoresis was utilized by Huang et al. in 2015 to synthesize LFP/G composite cathodes using suspended GO and commercial LFP [44]. These cathodes displayed capacities of 160 mAh/g at 0.1C and good rate performance, but required two thermal treatment steps to obtain the final LFP/G product. A unique LFP/G synthesis method developed by Shen et al. in 2015 used polyaniline to reduce GO mixed with LFP particles via redox reactions [45]. Their LFP/G composites exhibited fairly high rate performance and a capacity of up to 165 mAh/g at 0.2C. This synthesis method allows for precise control of carbon content without needing a secondary thermal treatment step. Similar findings were reported by Feng, Shen, and Guo in 2017 where pyrrole was used to reduce GO and form a LFP/G/polypyrrole composite [46]. Polymer membranes were utilized by Zhang et al. in 2016 to form graphene in-situ on LFP particles [47]. Resulting LFP/G composites had reversible capacities of almost 180 mAh/g at 0.1C, and 80 mAh/g at 10C. Raman spectrum analysis revealed that these composites had nearly equal levels of ordered and disordered carbon. Free-standing LFP/G composites were prepared by Wang et al. in 2018 by vacuum filtration of suspensions containing LFP particles and nanofibrillated cellulose [48]. These flexible composites had capacities of 150 mAh/g at 0.1C, and retained approximately 90%

capacity at a 0.1C rate after 1000 bends. These methods of synthesizing LFP/G are common in that samples prepared with both ordered and disordered carbon exhibited the highest capacities. Most preparation methods for LFP/G resulted in similar performance as long as good mixing between graphene precursors and LFP material was achieved.

The most important concept shared by these publications is that the method of incorporating graphene into LFP material is critical for obtaining increased electrochemical performance. Poor results were often obtained when graphene was added directly to LFP material or LFP precursors due to poor interaction between the two. By adding additional carbon, or by ensuring a good mixture between LFP precursors and graphene precursors, higher capacities and better rate performance was observed. Type of graphene precursor had a marginal impact on cell performance, but the most critical factor was mixing in the materials. Table 2.5.1-1 lists several notable LFP/G synthesis methods and the resulting capacity of the active materials.

Table 2.5.1-1 Summary of Research Discussed in Section 2.5.1.

Authors	Year	Notes	Active Material Capacity (mAh/g)
X. Zhou, F. Wang, Y. Zhu, Z. Liu [4]	2011	Added GO to LFP sol-gel precursors to form LFP/G	150 at 0.1C
C. Su, X. Bu, L. Xu, J. Liu, C. Zhang [42]	2012	Added graphene platelets to LFP sol-gel precursors to form LFP/G	140 at 0.1C
R. Mo, Z. Lei, D. Rooney, K. Sun [5]	2014	Added LFP precursors to GO suspended in water-oil emulsion, obtaining well integrated LFP/G.	160 at 0.1C
W. Shen, Y. Wang, J. Yan, H. Wu, S. Guo [45]	2015	Chemically reduced GO mixed with commercial LFP by the addition of polyaniline. Required no additional thermal treatment steps.	165 at 0.2C
Y. Zhang, Y. Huang, X. Wang, Y. Guo, D. Jia, X. Tang [47]	2016	Used electrospun polymer membrane as graphene precursor. Displayed very high reversible capacity.	180 at 0.1C

2.5.2 In-Situ Synthesis of Graphene from Humic Acid

As covered in previous sections, HA is capable of producing graphene under a variety of conditions. Graphene from HA has in some cases proven to be superior to

graphene made from other precursors and other synthesis routes. There exist several instances of HA's use in electrode materials for Li-ion batteries, but widespread use is not common. This can likely be attributed to the difficulties of obtaining HA in sufficient quantities and with a purity suitable for battery application. When HA has been incorporated into Li-ion battery electrode materials, increases in mechanical and electrical properties of the electrodes have been observed.

Graphitized carbon synthesized from HA was studied by Si et al. in 2018 where HA was carbonized at high temperatures and the resulting material used as active material in carbon-based LIB electrodes [33]. Purified HA was heated between 2200 °C and 2800 °C, forming thin graphitized carbon sheets which were used to make carbon anodes for a Li-ion cell. Electrodes prepared at 2800 °C exhibited a capacity of 239 mAh/g at a rate of 0.5C and 95% capacity retention after 50 cycles at 2C. The authors concluded that the 3D structure of the graphitized HA was suitable for lithium ion storage, performing significantly better than typical graphite electrodes. This research demonstrates that HA is a suitable graphene precursor material for the synthesis of LIB anode materials which perform better than standard graphite electrodes.

Another study conducted by Duraia et al. in 2018 looked to use HA to increase the mechanical strength and conductivity of tin oxide composite anodes [3]. Leonardite-derived HA was catalytically reduced to graphenol and added to tin oxide precursors. A schematic of their procedure is depicted in Figure 2.5.2-1. The resulting SnO₂-graphene composite exhibited capacities of 680 mAh/g and retained 80% of that capacity after 40 cycles, a significant improvement over standard tin oxide anodes. This performance was attributed to the ability of reduced HA to accommodate reversible volumetric changes

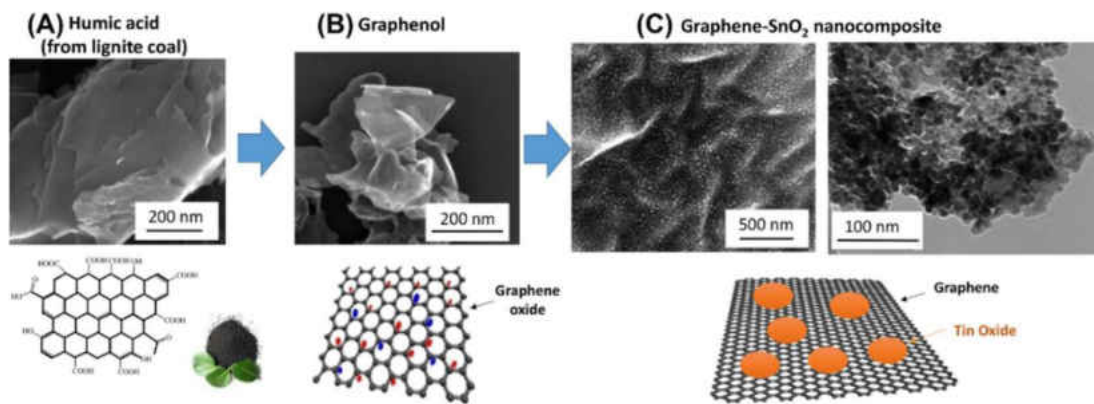


Figure 2.5.2-1 Schematic of Graphene-Modified Tin-Oxide Synthesis Process. Image credit to Duraia et al. [3].

that occur upon lithium ion insertion and de-insertion. This research builds on previous works by using HA as a graphene precursor to enhance the electrical and mechanical properties of composite electrode materials.

The application of HA as a graphene precursor in LIBs is still a relatively novel concept still undergoing research by various institutions. HA has proven effective as an alternative to GO which can improve the mechanical strength and electrochemical performance of electrodes for Li-ion cells as well as high performance capacitors [28]. The carbon structures formed after the reduction of HA lend themselves especially well to the facilitation of Li⁺ ion transport and their high conductivity makes them an ideal material for LIB applications. As understanding of HA grows, its use in highly technical applications such as high-performance LIB electrodes is expected to become more abundant. Table 2.5.2-1 provides a brief overview of the findings of the research covered in this section.

Table 2.5.2-1 Summary of Research Discussed in Section 2.5.2.

Authors	Year	Notes
D. Si, G. Huang, C. Zhang, B. Xing, Z. Chen, L. Chen, H. Zhang [33]	2018	Synthesized graphene-based anode materials with higher performance than common graphite electrodes.
E. M. Duraia, S. Niu, G. Beall, C. P. Rhodes [3]	2018	Enhanced electrical and mechanical properties of tin-oxide anode materials using HA.

3 **EXTRACTION OF HUMIC ACID**

3.1 Introduction

One of the largest hurdles preventing the use of HA in technical applications is obtaining HA in sufficient quantity with a minimal amount of impurities. The issue of quantity can be addressed by optimizing the HA extraction process to obtain a maximum yield. The extraction process can also have a slight impact on the level of impurities in the final HA product, however, there are several different methods to reduce impurities post-extraction. More on this can be found in Chapter 4: Purification of Humic Acid. Another important factor to consider is the material from which HA will be extracted. While materials such as soil, decayed plant matter, and coal contain moderate percentages of HA, oxidized coals and leonardite typically have some of the highest humic matter contents. North Dakota leonardite in particular is capable of having a HA content of up to 86% on a dry, ash-free basis [8]. North Dakota leonardite obtained from Leonardite Products, LLC of Williston ND was used as the raw material from which HA was extracted.

Several procedures for extracting HA from various materials exist, usually with the goal of obtaining some quantitative data on the amount of HA and FA present in the sample. In alkaline extraction, organic matter containing humic materials is treated with a basic solution, which dissolves the humic component. Solids are then separated from the solution by some mechanical means. The solution is then acidified, precipitating HA

while FA remains in solution. The IHSS method is based on this extraction mechanism, and lays out specific guidelines for acids and bases to use as well as solution concentrations and target pH values. For organic solvent extraction, an organic solvent is used to treat organic matter containing humic materials. HA is dissolved into the solvent, and then separated from undissolved solids. The solvent can then be evaporated leaving the extracted HA behind. These procedures generally do not take into account the amount of impurities that get extracted with the HA. Due to the desired end-use of the extracted HA in LIB applications, impurities were to be minimized while still retaining a high yield of HA. A series of experiments were designed based on literature data and our preliminary experiments. Extraction conditions for both alkaline and organic solvent procedures were then optimized based on criteria for obtaining HA suitable for use in LIBs with a high yield. Detailed information regarding optimized extraction procedure conditions is withheld to preserve the intellectual property of Clean Republic, LLC and the University of North Dakota.

3.2 Experimental Procedures

3.2.1 Optimizing Extraction Parameters/DOE Setup

Minitab statistical software was used to design experiments for both alkaline and organic extractions. These experiments were designed to test and verify procedures outlined in other various publications. Each set of experiments tested four factors at three different levels, with the exception of base type for alkaline extraction, for which only two bases were tested. In alkaline extraction, base type, solution concentration, solution to solids ratio, and extraction time were varied. Organic solvent to acid ratio, extraction temperature, solution to solids ratio, and extraction time were varied for the organic

extractions. An L9(3⁴) Taguchi design was used, resulting in nine total experiments for each extraction procedure. This design was selected in order to minimize the total number of experiments required while still maintaining adequate resolution for determining significant factors. Interactions between factors were not expected, nor encountered in previous literature, so a Taguchi design was determined to be suitable for the optimization of extraction conditions. Responses used to optimize extraction procedures included total yield of HA, ash content of the HA, as well as iron content, all on a dry mass basis. Yield was to be maximized while ash and iron content were to be kept to a minimum. Measurements of yield were on a dry mass basis as outlined in the IHSS extraction procedures [11]. Complete experiment tables with individual experiment results can be found below in Table 3.2.1-1 and Table 3.2.1-2. Experiments were conducted in a randomized order to rule out any effects that time may have on the results. Detailed information pertaining to the designed experiments and optimized parameters is withheld to preserve the intellectual property of Clean Republic, LLC and the University of North Dakota.

Table 3.2.1-1 Design of Experiment for Humic Acid Alkaline Extraction Conditions.

Experiment	Base	Concentration	Solution:Solid Ratio	Extract Time
1	B1	C1	L/S1	T1
2	B1	C2	L/S2	T2
3	B1	C3	L/S3	T3
4	B1	C1	L/S2	T3
5	B1	C2	L/S3	T1
6	B1	C3	L/S1	T2
7	B2	C1	L/S3	T2
8	B2	C2	L/S1	T3
9	B2	C3	L/S2	T1

Table 3.2.1-2 Design of Experiment for Humic Acid Organic Solvent Extraction Conditions.

Experiment	Solvent/Acid Ratio	Solution:Solid Ratio	Temperature	Extract Time
10	S/A1	L/S1	Tmp1	T1
11	S/A1	L/S2	Tmp2	T2
12	S/A1	L/S3	Tmp3	T3
13	S/A2	L/S1	Tmp2	T3
14	S/A2	L/S2	Tmp3	T1
15	S/A2	L/S3	Tmp1	T2
16	S/A3	L/S1	Tmp3	T2
17	S/A3	L/S2	Tmp1	T3
18	S/A3	L/S3	Tmp2	T1

3.2.2 Materials and Methods

Material from which the HA was extracted was obtained from Leonardite Products, LLC of Williston, North Dakota. The specific product, Source Fines, was dried at 105 °C until no change in mass was observed over a period of several hours.

Extractions were carried out in sealed beakers for each test. Separation of liquid phase and solids was done by centrifuging with an Eppendorf 5810 centrifuge. Dilute acid was used to precipitate HA from alkaline extraction solutions. Organic solvents used to extract HA were removed by evaporation at reduced pressure. Extracted HA was washed with de-ionized water to remove residual salts. Washed HA was then dried at 105 °C. The dried mass of HA was compared to the mass of leonardite used for the extraction to determine percent yield on a dry mass basis.

3.2.3 Materials Characterization

Elemental compositions of leonardite and humic acids were determined by X-ray fluorescence (XRF) on a Rigaku Supermini 200. Ash content was determined using

ASTM D3174-12, Standard Test Method for Ash in the Analysis Sample of Coal and Coke from Coal.

3.3 Results and Discussion

Conditions for both extraction procedures were optimized based on maximizing the yield of HA with the highest overall purity and lowest iron content. These values were used as responses for the designed experiments and were input back into Minitab in order to determine optimum conditions.

The leonardite starting material was tested in the same manner in order to compare the level of impurities and iron content to the extracted HA. Ash content was determined to be 20.9% on a moisture-free basis. XRF elemental composition by mass percent is shown below as Table 3.3-1. There is a large amount of both iron and silicon in the leonardite material, among other impurities. The value for organic material also includes all organic matter, both humic and non-humic.

Table 3.3-1 XRF Elemental Composition of Leonardite Products Source Fines. All values are in mass percent.

Component																		
Na	Mg	Al	Si	P	S	Cl	K	Ca	Ti	Cr	Mn	Fe	Zn	As	Sr	Zr	Ba	Organic
0.146	0.686	1.568	2.062	0.010	1.001	0.019	0.193	0.792	0.060	0.005	0.035	2.516	0.006	0.005	0.015	0.001	0.185	90.696

3.3.1 Alkaline Extraction

Results for the alkaline experiments are shown in Table 3.3.1-1. It can be seen that to a degree, yield and iron content are directly related, as samples with higher yields had more iron and vice versa. Purity exhibits a similar correlation with yield, but not to the same extent that iron content does. It is also noted that the yields fall short of some of

the literature-reported values. This is due to testing a single-pass style extraction versus exhaustive or multiple-pass style extractions used in some publications.

Table 3.3.1-1 Yield, Overall Purity, and Iron Content for Alkaline Extraction DOE.

Experiment	Base	Concentration	Solution:Solid Ratio	Extract Time	Yield	Purity	Iron Content
1	B1	C1	L/S1	T1	4.0%	98.1%	0.9%
2	B1	C2	L/S2	T2	24.1%	97.2%	1.5%
3	B1	C3	L/S3	T3	44.4%	97.3%	0.8%
4	B1	C1	L/S2	T3	10.6%	96.2%	1.5%
5	B1	C2	L/S3	T1	29.7%	96.5%	1.5%
6	B1	C3	L/S1	T2	38.6%	97.5%	1.3%
7	B2	C1	L/S3	T2	15.1%	97.0%	1.4%
8	B2	C2	L/S1	T3	31.1%	96.8%	1.7%
9	B2	C3	L/S2	T1	52.1%	95.9%	1.5%

Yield of HA was the first factor considered as a response, and a main effects chart is shown as Figure 3.3.1-1. From the figure it is clear that solution concentration has the largest effect on yield due to its vertical span. Base type, solution to solids ratio, and then extraction time followed in terms of impact on HA yield. Highest yields were

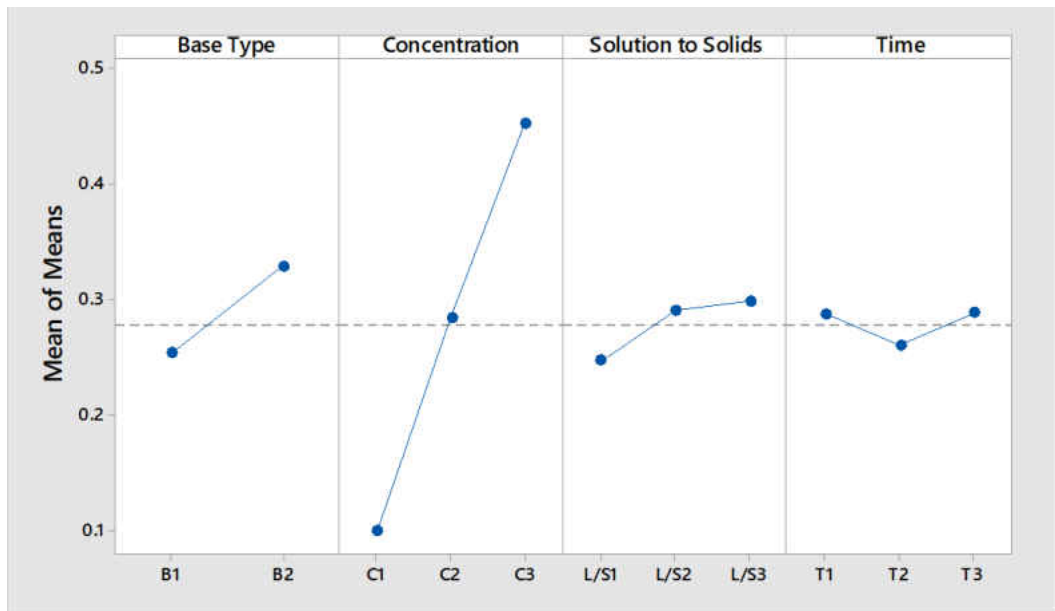


Figure 3.3.1-1 Main Effects Plot for Alkaline Extraction DOE with Yield as Sole Response.

obtained at the highest solution concentrations tested. It could be assumed that increasing the concentration of the base in solution should increase the amount of HA extracted up to a point; however, previous works have found that too strong of basic concentrations can cause chemical alteration of the extracted humic materials [49-51]. Base type had the second largest impact on HA yield, with base 2 having the highest yield. Liquid to solids ratio was the third-most significant factor effecting yield, with the best results seen at L/S3. The difference in yield between L/S2 and L/S3 is small enough that a significant gain in extracted HA would not be expected at higher solution to solid ratios. The most insignificant of the factors tested was time. The inverse peak on Figure 3.3.1-1 pertaining to time, and the relatively low vertical spread between the points indicates that extraction time has little effect on the total yield of HA.

Overall purity was the second response used to optimize the alkaline extraction procedure. Figure 3.3.1-2 is the main effects plot for when overall purity is used as the response for the alkaline extraction DOE. The ratio of solution to solids had the largest effect on the overall purity of HA obtained by alkaline extraction. HA extracted with the lowest solution to solids ratio exhibited the highest overall purity by far. Lower ratios were not tested as the amount of HA recovered was too small to be useful in most capacities. Base type had the second largest impact on overall purity, with base 1 yielding the best results. Extraction time followed as the having the third most significance, with a moderate extraction time of T2 resulting in the highest purities. Lower solution concentrations were not tested due to issues with lower yields of HA or needing much larger quantities of extracting solution.

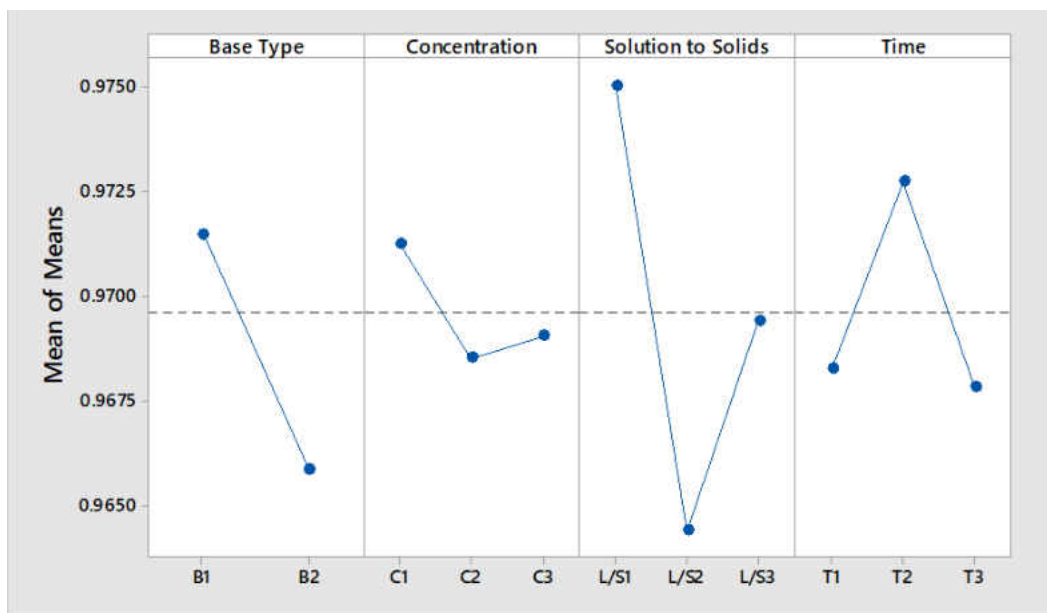


Figure 3.3.1-2 Main Effects Plot for Alkaline Extraction DOE with Overall Purity as Sole Response.

Iron content was the third response considered for optimizing the alkaline extraction conditions. Iron in particular has a significantly negative impact on LFP electrode materials, so it is desired to be minimized in any LFP additives. Figure 3.3.1-3 is a main effects plot for the alkaline extraction DOE with iron content as the response. Considering iron content as the response, the most significant factor is concentration, with the highest concentration tested yielding the best results. Again, further increasing solution concentration is not desired as that will change the structure of HA. Solution to solids ratio had the second largest impact, with the L/S3 ratio resulting in the lowest iron content. Higher solution concentrations and solution to solids ratios were not tested due to reasons outlined above. Base 1 tended to result in lower iron concentrations compared to base 2, and was the third most significant factor. Time was the fourth most significant factor effecting iron content. The low vertical deviation and the upward pointing peak indicate extraction time has little effect on iron content.

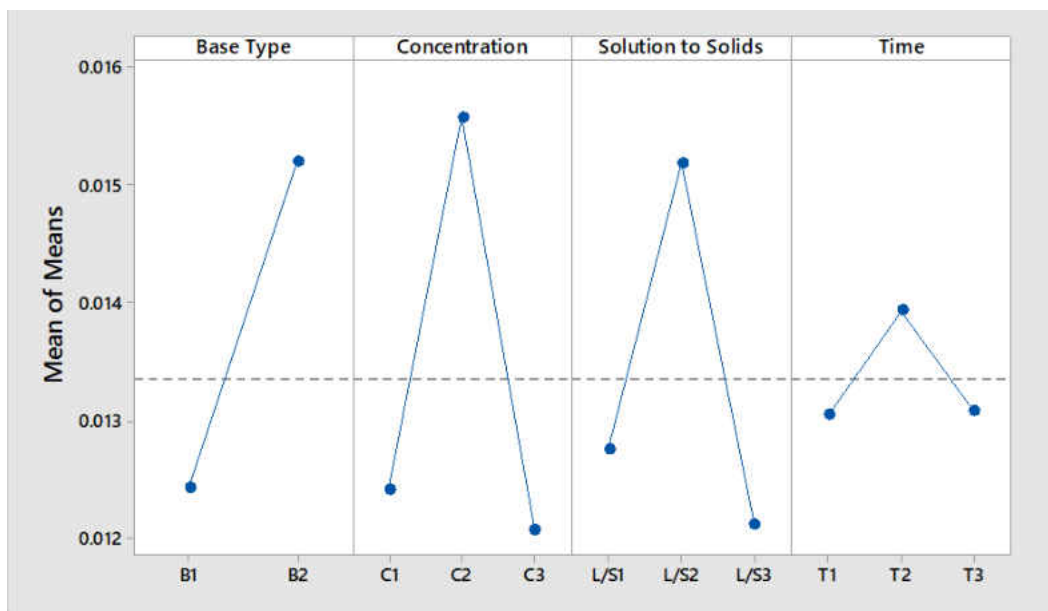


Figure 3.3.1-3 Main Effects Plot for Alkaline Extraction DOE with Iron Content as Sole Response.

The rank of importance for each factor was determined based on the ability of a factor to influence a particular response. These factor weights were then used along with observations during the experiments to determine the optimum conditions for the alkaline extraction of HA. Table 3.3.1-2 lists the optimum conditions and factor ranks for each response. In cases where two levels for a certain factor yielded similar results, both were listed with the better performing level first.

Table 3.3.1-2 Alkaline Extraction Optimum Conditions and Ranks per Response.

Response	Base Type	Rank	Concentration	Rank	Soution to Solids	Rank	Time	Rank
HA Yield	B2	2	C3	1	L/S3/L/S2	3	T1/T3	4
HA Purity	B1	2	C1	4	L/S1	1	T1/T3	3
Iron Content	B1	3	C3/C1	1	L/S3/L/S1	2	T1/T3	4

Based on Table 3.3.1-2, concentration of base in the extract solution seems to be the most significant factor, and extract time the least. Solution to solids ratio and base

type are both of moderate significance, with the former having a slightly higher impact on the responses overall. Base types were fairly even, with base 1 having a slight edge when considering iron content of the extracted HA. Also, base 2 has a slight disadvantage due it forming more salts which require a more intensive washing regime to remove. A solution concentration of C3 was most effective for all responses except overall HA purity, on which the concentration factor had the least effect. For solution to solids ratio, the optimal ratio was L/S1, however in a few of the experiments this proved to be insufficient to fully wet the leonardite which was undergoing extraction. For this reason, the second-best solution to solids ratio, L/S3 was selected as the optimal condition. Lastly, extraction time was of little importance when each of the factors was considered. Extraction times T1 and T3 often yielded similar results, so T1 was selected as the optimum extract time as it was the shorter of the two and more suitable for rapid extractions.

Findings of the designed experiment as well as observations in the lab indicate that the optimal conditions for HA alkaline extraction are: base type of B1 with a concentration of C3, in a solution to solids ratio of L/S3 and an extract time of T1. Minitab was then utilized to estimate the values for each response given these conditions. Table 3.3.1-3 lists the predicted results and the actual results obtained in the lab for the extraction performed using the optimized parameters.

Table 3.3.1-3 Comparison of Minitab Predictions vs. Lab-Obtained Results from Optimized Alkaline Extraction Procedure. Values are in mass percent.

	Yield	Iron Content	Overall Purity
Minitab Predicted Results	45.3%	1.0%	96.9%
Observed Results	44.2%	1.3%	97.0%

The HA extracted using the optimized alkaline extraction procedure was very close to meeting all of the attributes that Minitab predicted based on the DOE results. Yield and iron content fell just short of their estimated values, and overall purity was just about a perfect match. These results indicate that the estimated values for yield, iron content, and overall purity are achievable, and these optimized conditions can be used for subsequent HA extraction.

3.3.2 Organic Solvent Extraction

Results of the organic solvent extraction DOE are shown in Table 3.3.2-1. Overall yields of HA were significantly lower for the organic solvent extraction compared to the alkaline extraction procedure. Iron content was fairly consistent, with one experiment attaining an iron content lower than all alkaline extraction experiments, although experiment 18 exhibited extraordinarily high iron numbers. This was thought to be due to an error in the experiment, but a repeat resulted in similar results in all three responses.

Table 3.3.2-1. Yield, Overall Purity, and Iron Content for Organic Solvent Extraction DOE.

Experiment	Solvent/Acid Ratio	Solution:Solid Ratio	Temperature	Extract Time	Yield	Purity	Iron Content
10	S/A1	L/S1	Tmp1	T1	37.0%	95.5%	3.0%
11	S/A1	L/S2	Tmp2	T2	32.8%	97.7%	1.2%
12	S/A1	L/S3	Tmp3	T3	37.8%	97.6%	1.4%
13	S/A2	L/S1	Tmp2	T3	35.0%	93.7%	4.7%
14	S/A2	L/S2	Tmp3	T1	28.8%	97.8%	1.1%
15	S/A2	L/S3	Tmp1	T2	19.6%	98.2%	0.8%
16	S/A3	L/S1	Tmp3	T2	6.8%	97.9%	1.0%
17	S/A3	L/S2	Tmp1	T3	12.9%	98.4%	0.8%
18	S/A3	L/S3	Tmp2	T1	10.6%	92.3%	6.1%

Yield was again considered as the first response for optimizing the organic extraction procedure. Figure 3.3.2-1 shows the effect of solvent to acid ratio, extraction

temperature, solution to solids ratio, and extraction time have on yield of HA obtained by organic solvent extraction. It is apparent from the figure that solvent to acid ratio is most

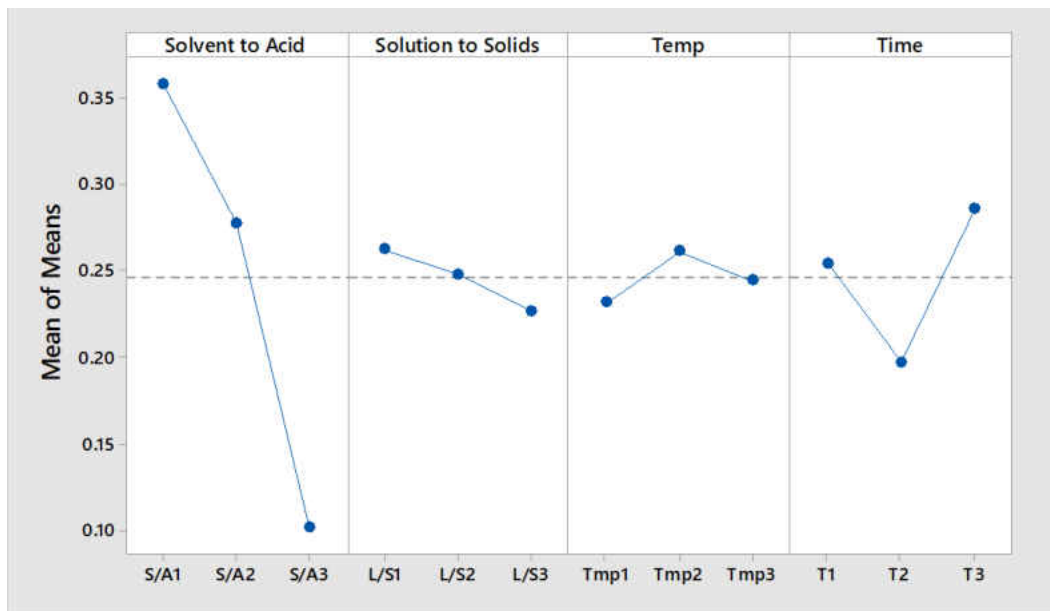


Figure 3.3.2-1 Main Effects Plot for Organic Solvent Extraction with Yield as Sole Response.

significant, followed by extract time, solution to solids ratio, and extract temperature. The solvent to acid ratio for organic solvent extraction has the largest impact on yield of HA. Highest yields were obtained at the lowest solvent to acid ratios, which is likely due to HA's insolubility in acidic conditions. The trend of solvent to acid ratio would indicate that further reduction in acid would lead to a higher yield of HA, however S/A1 was approximately the minimum amount of acid required to replace metal ions in the HA sample with hydrogen [14, 15]. Extraction time had the second largest impact on yield, however as seen in the alkaline extraction experiments, there is not a clear correlation between extraction time in the tested range and HA yield. Higher yields of HA were seen with an extraction time of T3. Solution to solids ratio for the extractions was the third

most influential factor effecting HA yield. The best yields were seen at the solution to solids ratio of L/S1. The data suggests that as the amount of extracting solution decreases, the yield of HA increases, which is the opposite of what was expected. Temperature exhibited the least impact on HA yield, with the best results obtained at the Tmp2 temperature value.

The overall purity of HA obtained by organic solvent extraction was the second response considered for optimizing extraction conditions. Figure 3.3.2-2 is a main effects plot for the organic extraction with overall HA purity as the response. The factor with the

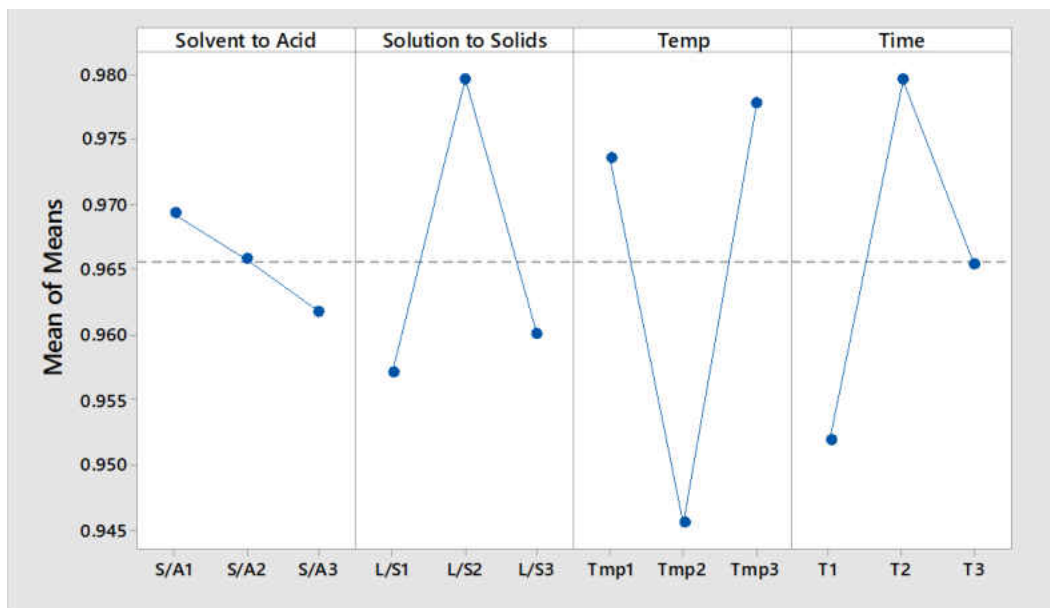


Figure 3.3.2-2 Main Effects Plot for Organic Solvent Extraction with Overall Purity as Sole Response.

most prominent effect on overall purity of the extracted HA was extraction temperature. Temperature Tmp2 resulted in the highest levels of impurities, while Tmp3 yielded the least. Higher extraction temperatures were not tested, as Tmp3 was already approaching the boiling point of the organic solvent used. Extraction time had the second largest effect

on overall HA purity, with the time T2 having the best results. Solution to solids ratio had the third largest impact. The ratio L/S2 proved to be far more effective at extracting HA with low impurities than the L/S1 and L/S3 ratios. The factor that had the least impact on the purity of extracted HA was the solvent to acid ratio. The ratio which had the best results was S/A1. The upward trend in HA purity as acid content decreases was unexpected, as a few sources mentioned the need for acid to fully remove metal ions from the HA [14, 15].

Figure 3.3.2-3 shown below is the main effects plot for the organic solvent extraction considering iron content as the response. When iron content was considered

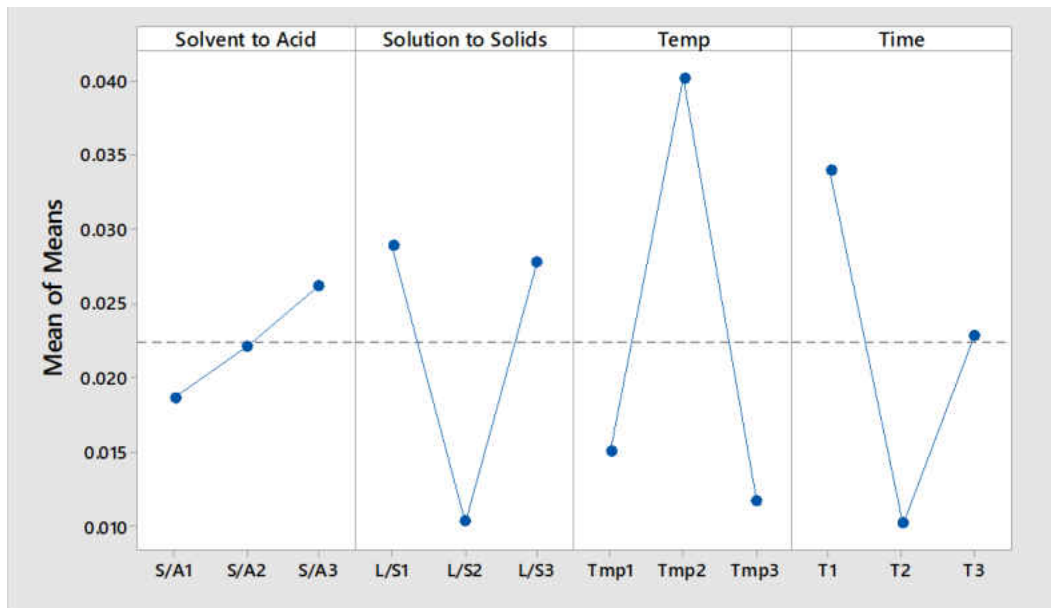


Figure 3.3.2-3 Main Effects Plot for Organic Solvent Extraction with Iron Content as Sole Response.

for the optimization of the organic solvent extraction process, the results mirrored those for when overall purity was considered as the response. Temperature had the largest effect iron content as well, with the best results obtained at Tmp3 and Tmp1. The factor

with the second highest impact was extraction time. Time T2 resulted in the lowest iron content. Solution to solids ratio was the third most significant factor, with iron content being minimized at the ratio L/S2. Solvent to acid ratio was the least significant factor, with iron minimized at the value of S/A1.

The rank of importance for each factor was determined based on the ability of a factor to influence a particular response. These factor weights were then used along with observations during the experiments to determine the optimum conditions for the organic solvent extraction of HA. Table 3.3.2-2 lists the optimum conditions and factor ranks for each response. In cases where two levels for a certain factor yielded similar results, both were listed with the better performing level first.

Table 3.3.2-2 Organic Solvent Extraction Optimum Conditions and Ranks per Response.

Response	Solvent to Acid Ratio	Rank	Solution to Solids	Rank	Temperature	Rank	Time	Rank
HA Yield	S/A1	1	L/S1	3	Tmp2	4	T3	2
HA Purity	S/A1	4	L/S2	3	Tmp3/Tmp1	1	T2	2
Iron Content	S/A1	4	L/S2	3	Tmp3/Tmp1	1	T2	2

The results shown in Table 3.3.2-2 indicate that temperature has the largest total effect on yield, overall purity, and iron content for organic solvent extraction. The best overall temperature condition is Tmp3. Extraction time is the second most influential overall factor, with T2 being the optimal time. Solution to solids ratio has the third largest effect on all three factors. The solution to solid ratio L/S2 was selected as it was the best level for two of three responses, and the L/S1 ratio was at times insufficient to fully wet the leonardite material. Solvent to acid ratio had the lowest average impact out all of the factors, with the ratio S/A1 being the universal best condition.

Based on the results of the designed experiment and observations in the lab, the optimized conditions for organic solvent extraction of HA are at: a solvent to acid ratio of S/A1, Liquid to solids ratio of L/S2, temperature Tmp3, and extract time T2. These conditions were then input back into Minitab and predictions for each response were obtained. Table 3.3.2-3 compares the Minitab predicted results to those obtained in the lab using the optimized organic extraction parameters.

Table 3.3.2-3 Comparison of Minitab Predictions vs. Lab-Obtained Results for Optimized Organic Solvent Extraction Procedure. Values are in mass percent.

	Yield	Iron Content	Overall Purity
Minitab Predicted Results	31.1%	0.0%	100.0%
Observed Results	31.4%	1.2%	97.7%

The obtained results were in fairly good agreement with the values predicted by Minitab. While the predicted values for iron content and overall purity were not practical, the lab results were not too far off. Yield was almost equivalent to what was expected, with iron content being slightly higher and purity being slightly lower than what was predicted. These results were very similar to experiment 11, which differed only in extraction temperature. Both sets of conditions resulted in an acceptable yield of HA with low iron content and good purity.

3.3.3 Comparison of Extraction Methods

When comparing the two extraction methods tested, multiple considerations need to be taken into account in addition to the responses considered for the experiments. The alkaline extraction procedure resulted in the best overall results for yield, with iron content and overall purity being only slightly worse than those obtained by the organic solvent extraction procedure. Table 3.3.3-1 compares the optimized conditions and

responses for each extraction method. Results for yield, iron content, and overall purity are in mass percent. It can be observed that that the alkaline extraction procedure is

Table 3.3.3-1 Comparison of Optimized Conditions and Extraction Results for Alkaline and Organic Solvent Procedures. Values for responses are in mass percent.

	Solution to solids ratio	Extraction Time	Base Type	Base Concentration	Solvent to acid ratio	Temperature	Yield	Iron Content	Overall Purity
Alkaline Extraction	L/S3	T1	B1	C3	n/a	n/a	44.2%	1.3%	97.0%
Organic Solvent Extraction	L/S2	T2	n/a	n/a	S/A1	Tmp3	31.4%	1.2%	97.7%

favorable in terms of extracting an acceptable mass of HA from leonardite, while the organic solvent process has a slight edge as far as iron content and overall purity of the extracted HA. Both processes are theoretically suitable for scaling to pilot or production scale processes. A larger scale process for producing HA via the alkaline process may have high capital costs due to needing materials to handle the wide variation in pH, and fresh acid and bases would be required for continuous operation. A production-scale organic solvent extraction process would be complicated with equipment necessary for handling large amounts of flammable solvents and vapors. Taking these characteristics into consideration, neither extraction method has an advantage over the other as far as scalability. The alkaline extraction procedure may have a slight edge if fractionation of HA was desired in a production-scale process, as it may be possible to utilize pH control to obtain fractions of HA differing in molecular size [49]. Another consideration has to do with the selectivity of the organic solvent method with regards to HA and FA. HA obtained via organic solvent extraction typically had a lighter brown color than the black color of HA obtained via alkaline extraction. This suggests the organic solvent extraction may be extracting lighter weight fulvic compounds along with the HA. This is not necessarily a downside, but heavier weight HA fractions are more desired for graphene

formation. If FAs are indeed extracting in the organic solvent method, that would mean that the amount of HA extracted is actually less than observed. Considering these characteristics of the two extraction methods, it would seem that the alkaline extraction method exhibits a slight edge over the organic solvent extraction procedure, and may be better suited to a production-scale process.

3.4 Conclusion

Based on the results of several experiments designed around two different HA extraction methods, an optimized procedure for extracting HA from leonardite has been developed. Experimental conditions for both alkaline and organic solvent extraction methods were varied and the results examined to develop a set of conditions which yielded a sufficient amount of HA with good purity and low iron content. The alkaline extraction process yielded 44.2% HA by mass with an iron content of 1.3% and a purity of 97.0%. The organic solvent extraction resulted in HA with a yield of 31.4% containing 1.2% iron and having a purity of 97.7%. The two optimized extraction methods were then compared and the alkaline extraction procedure selected as the ideal technique for obtaining HA from leonardite.

4 PURIFICATION OF HUMIC ACID

4.1 Introduction

There exist several procedures for extracting humic material from soil and decayed organic matter, however none of them are capable of producing a pure HA product. Because of this, additional purification steps are often required to reduce impurities to levels suitable for use in highly technical applications such as battery electrode materials. Major impurities that remain in HA after extraction include silicates, residual salts, and metals complexed with organic matter. Purification procedures included in this chapter will cover the removal of these types of impurities.

Silicates are minerals present in organic matter such as coal and leonardite. They are inorganic crystals which remain as ash upon combustion, and are otherwise an impurity. The low solubility and relatively low reactivity of silicates can often be exploited to facilitate their removal by physical means such as filtration. In both the alkaline and organic solvent extraction procedures detailed in Chapter 3, HA is dissolved into solution to allow physical separation from non-humic material and inorganics. Using filters with a small particle retention size has shown to reduce ash to acceptable levels. Centrifuging has also proven to be efficient at removing silicates provided the relative centrifugal force (rcf) is high enough to settle out fine particles. Chemical removal of silicates is possible only through the use of hydrofluoric acid (HF), which is able to attack and dissolve the silicate crystals. Mineral acids are commonly used in conjunction with

HF in order to weaken ionic silicate bonds and facilitate its complete removal [25, 52]. This purification process has been tested on HA, yielding a product with reduced ash content [17].

Alkaline and organic solvent HA extraction procedures both utilize acid which can cause the formation of salts in solution. These salts, often in the form of metal-chlorides, can remain embedded in the extracted material as an impurity if not properly removed. Typically, these salts can be removed by rinsing the HA with a sufficient amount of de-ionized water, which can also aid in ash reduction [11, 12, 17].

Iron is present in organic matter and humic-containing material primarily in two forms. Pyrite is a major source of iron and sulfur, both of which are significant impurities. Pyrite is insoluble in both of the extraction methods examined, so it can be removed in the same manner as silicates, through filtering or centrifuging. The other major source of iron in HA is from organic-metallic complexes. These complexes are formed by multiple ionic bonds between metal ions and carboxyl groups, and can be difficult to break up. Typically, complexes such as these can be disrupted through the use of a strong chelating agent. Desirable chelating agents used to reduce metallic impurities can form strong organic-metallic complexes and are soluble in low pH conditions, facilitating the efficient separation and removal of HA [25]. Additionally, a chelating agent which will not introduce impurities if not entirely removed is also desired. Specific information pertaining to the type of chelating agent and the experimental conditions are withheld to preserve the intellectual property of Clean Republic, LLC and the University of North Dakota.

4.2 Experimental Procedures

Generally, the overall purification process was as follows: i) insoluble material is separated from HA in solution using either filtering or centrifuging, ii) extracted HA is washed with de-ionized water, iii) a chelating agent is used to reduce iron and other metallic cations that are present, and iv) a mineral acid mixture is used to further reduce ash and silicates. HA obtained after purification is always washed with de-ionized water to ensure the removal of salts which may be present as a result of the extraction and purification procedures. Specific information pertaining to specific materials and experimental conditions used is withheld to preserve the intellectual property of Clean Republic, LLC and the University of North Dakota.

4.2.1 Ash and Silicate Removal

Physical removal of ash and silicates was conducted while HA was in solution for both extraction methods tested. Silicate and ash removal by filtration was done by vacuum filtering the HA-containing solutions through progressively smaller nylon mesh filters. The smallest filter size used had a pore size of a few microns. Centrifuging was also used for silicate removal, by centrifuging the HA-containing solutions at a high rcf for several minutes, and then carefully decanting the liquid.

Chemical removal of silicates and ash was done using a procedure similar to that of Piccolo [17]. Hydrated HA was mixed with a dilute mineral acid solution and allowed to stir for at least 24 hours. The HA was then collected by centrifuging, and washed to remove residual salts. Typically, the acid treatment was done as the last purification step after treatment with a chelating agent, and only if necessary.

4.2.2 Removal of Residual Salts

Both the alkaline and the organic solvent extraction procedures optimized in Chapter 3: Extraction of Humic Acid also include a washing step to reduce residual salt content. Extracted HA was mixed with de-ionized water and stirred before collecting by centrifuging. This was repeated several times to ensure a minimum quantity of salts remained.

4.2.3 Removal of Iron and Other Metallic Impurities

A strong chelating agent was utilized to remove iron and other ion-form impurities from HA. The HA was dissolved in solution, and the chelating agent added. Solution pH was then manipulated to a value optimal for iron-chelate formation [26]. After stirring for a sufficient amount of time, pH was again manipulated to facilitate the collection of HA. HA was then collected by centrifuging and washed with de-ionized water.

4.2.4 Materials Characterization

Elemental compositions of samples were determined by X-ray fluorescence (XRF) on a Rigaku Supermini 200. Ash content was determined using ASTM D3174-12, Standard Test Method for Ash in the Analysis Sample of Coal and Coke from Coal.

4.3 Discussion

The various purification treatments tested all worked to varying degrees with different benefits and drawbacks. Factors such as ability to scale and effectiveness were considered when determining which treatments were adequate to obtain HA that had a

purity suitable for technical use. The following sections cover the removal of specific impurities.

4.3.1 Ash and Silicate Removal

Physical removal of ash and silicates was accomplished by filtering or centrifuging the solution which contained dissolved HA. Silicon content as well as total ash for samples of HA extracted by alkaline procedure at lab scale and collected by filtration or centrifuge are compared in Table 4.3.1-1. Filtering HA is quite effective at removing ash, however, it can be a time-consuming process. Hydrated HA is similar to a

Table 4.3.1-1 Silicon and Ash Contents of Filtered and Centrifuged Humic Acid Samples. Values are in mass percent.

Sample	Silicon	Ash
Filtered HA	0.12%	0.48%
Centrifuged HA	0.38%	2.00%

thick gel which is rather difficult to filter. Sequential filtration through progressively more restrictive filters is often required to prevent build-up of insoluble material and filter blockage. Centrifuging is also an effective way to remove silicates and other insoluble material. Care must be taken, as it is possible for solids to be carried away with the liquid when decanting the samples. This is reflected in Table 4-3.1-1, with the centrifuged HA sample having higher silicon and ash contents.

Lab scale HA extraction benefits from centrifuging as it is faster than filtration. On a larger scale, the best options for separating insoluble from HA-containing solution are likely to be a type of continuous, positive pressure filtration, or by continuous centrifuging. Both of these options would result in reduced liquid-solid separation time,

and eliminate issues with the re-suspension of solids observed with lab-scale centrifuging.

Chemical removal of silicates by acid treatment was successful as evident by the reduction in silicon and ash content in Table 4.3.1-2. HA that was chemically treated to

Table 4.3.1-2 Silicon and Ash Contents of Humic Acid Before and After Acid Treatment. Values are in mass percent.

Sample	Silicon	Ash
HA Before Acid Treatment	0.67%	2.79%
HA After Acid Treatment	0.53%	1.69%

remove ash and silicates was obtained at pilot scale by alkaline extraction, and had been previously treated with a chelating agent to reduce metal ions. This sample exhibits a higher ash content than would be expected based on the optimized extraction conditions, however this HA was extracted in a pilot scale batch of several kilograms before the pilot scale process had been fine-tuned. Ash content was reduced from 2.79% wt. in the HA treated with a chelating agent, to 1.69% wt. after acid treatment. XRF analysis indicated a slight reduction in silicon content from 0.67% wt. to 0.53% wt. The main drawback to using the acid mixture is the specialized equipment required to handle HF and the additional hazards it poses over silicate removal methods. Scaling up the acid treatment procedure would likely not be beneficial as the reduction in silicon and ash is not significant compared to the added complexity and hazards of dealing with HF. Alternatively, careful filtering during the extraction step can result in low silicon and ash contents, rendering the acid treatment step unnecessary.

The chelating agent used to reduce iron and other metal impurities has also resulted in a reduction of ash. Bonds between the humic matter and ash particles are

thought to be weakened due to the use of the chelating agent, thereby facilitating their removal. Table 4.3.1-3 lists the ash content for untreated HA that was extracted by an early pilot-scale procedure as well as the same HA that has been treated with a chelating agent. Ash contents as low as 0.12% have been observed with very high concentrations of

Table 4.3.1-3 Ash Contents of Humic Acid Before and Treatment with Chelating Agent. Values are in mass percent.

Sample	Ash
HA Before Chelating Agent Treatment	4.50%
HA After Chelating Agent Treatment	2.79%

chelating agent, however separation of the agent and HA proved difficult. The concentration of chelating agent used is an aspect of the purification procedure that could be optimized to potentially further reduce ash and metallic impurities.

4.3.2 Removal of Residual Salts

Residual salt removal is an effective way to decrease the amount of impurities in HA that are left behind as a byproduct of acid use in the extraction process. Table 4.3.2-1 displays XRF elemental composition results of a HA sample before and after washing with DI water. It is quite apparent that a simple wash step can significantly reduce the

Table 4.3.2-1 Elemental Compositions of Pre-wash and Washed Humic Acid. Values are in mass percent.

Sample	Component													HA
	Na	Al	Si	P	S	Cl	K	Ca	Ti	Fe	Cu	Zr		
Pre-wash HA	---	0.084	0.054	---	0.458	2.286	0.032	---	0.046	0.226	0.004	0.002	96.809	
Washed HA	0.033	0.106	0.071	0.005	0.545	0.199	0.034	0.007	0.042	0.191	0.004	0.002	98.760	

amount of impurities in HA. Chlorine was most the prominent impurity, and was reduced from about 2.29% to less than 0.20% in the sample. A small increase in lighter elements

is attributed to the amount of Cl that was removed causing an increase in the relative mass percent in the washed HA sample.

4.3.3 Removal of Iron and Other Metallic Impurities

Iron removal was achieved through both physical removal of pyrite, and through the disruption of organic-metallic complexes. Pyrite removal was achieved through filtration and centrifuging, the same methods used to physically remove silicates. Centrifuge was the primary method for minimizing impurities due to pyrite. Removal of complexed iron was achieved by the use of a strong chelating agent. Solution pH was controlled when the chelating agent is added in order to convert the organic-metal complexes into chelated metal compounds. Resulting metallic chelates are soluble at low pH values, making their removal from HA simple. This treatment is also quite suitable for scaling up, as the process is relatively straight forward and simplistic, and can be done immediately after extraction. Table 4.3.3-1 displays the elemental composition of a HA sample before and after treatment with the chelating agent. The chelating agent treatment

Table 4.3.3-1 Elemental Compositions of Humic Acid Sample Before and After Treatment with Chelating Agent. Values are in mass percent.

Sample	Component																HA
	Mg	Al	Si	P	S	Cl	K	Ca	Ti	Cr	Fe	Ni	Cu	Zn	Zr	Mo	
Untreated HA	---	0.263	0.418	0.005	0.330	0.022	0.937	---	0.047	0.042	0.835	0.010	0.008	0.010	0.003	0.001	97.069
Chelating Agent Treated HA	0.011	0.393	0.673	0.004	0.457	0.259	0.149	0.005	0.062	0.039	0.090	---	0.007	---	0.002	---	97.851

was able to significantly reduce the amount of iron in the sample. HA purified using the chelating agent was obtained via an early pilot-scale extraction, and as such had a relatively high amount of ash in the sample. The HA sample before treatment contained 0.835% iron on a dry mass basis, which was reduced to 0.090% by the chelating agent, meaning nearly 90% of the iron was removed by this treatment step.

There exist other ways for chemically removing iron and other metallic impurities which are popular for upgrading coal. These methods often require the use of mineral acids or other strong oxidizers to remove the impurities. These can oxidize and cause chemical changes to the HA structure, which is undesired. For this reason, these metallic impurity reduction techniques were not pursued in this study.

4.4 Conclusion

While an extraction procedure which produces pure HA has yet to be developed, there are several techniques which may be employed to reduce various the impurities. Both silicate and pyrite particles can be kept to a minimum by the use of sequential filtration or centrifuging during the HA extraction step. Vacuum filtering was able to reduce ash below 0.50%, but is not suited for large-scale HA production due to the gelatinous nature of hydrated HA which makes filtration difficult. Chemical removal of silicates and ash is possible by using a mineral acid mixture, although improvement was only marginal compared to the other techniques tested. Washing extracted HA with de-ionized water has proven to be effective at removing residual salts and was able to reduce chlorine content from 2.29% to less than 0.20% for one sample. A strong chelating agent is necessary to remove iron and other metal ions from HA, and was found to reduce iron by almost 90%. By utilizing the optimized extraction procedure and the purification techniques covered in this chapter, obtaining high purity HA for technical applications is possible.

5 GRAPHENE-MODIFIED LITHIUM IRON PHOSPHATE SYNTHESIS AND ELECTROCHEMICAL TESTING

5.1 Introduction

LIBs prepared with LFP cathodes benefit from intrinsic stability and safety, long lifespan, and low environmental impact but suffer low conductivity in the active material, making LFP an excellent material for modification with graphene. Graphene modified LFP, (LFP/G) benefits from increased conductivity, better high-rate performance, elevated specific capacity, as well as enhanced mechanical properties. These improvements can make LFP/G an attractive alternative to commercial LFP cathode materials.

To test the initial concept of forming an LFP/G composite using HA, an LFP/G synthesis method was tested based on mixing dry precursor materials with HA. Performance of active material synthesized by this procedure was not expected to be as good as material synthesized by other methods which incorporate better mixing, although the produced active material should give an indication on how the LFP precursors and HA interact upon thermal treatment.

Another LFP/G synthesis method tested was developed jointly between Clean Republic, LLC and the University of North Dakota. This proprietary process for incorporating HA into LFP ensures excellent crystal purity and molecular level mixing. The procedure is based off of modifications to their previous LFP synthesis process, and

as such remains confidential. Detailed information regarding the LFP/G synthesis procedure is withheld to preserve the intellectual property of Clean Republic, LLC and the University of North Dakota.

5.2 Experimental Procedures

5.2.1 LFP/G Synthesis

LFP/G was first synthesized by mixing dried LFP precursor material with dried HA. LFP precursor material was synthesized via sol-gel method using equal molar amounts of lithium acetate (Acros, 199842500), phosphoric acid (Fisher, A242-212), and iron nitrate nonahydrate (Aldrich, 216828). The precursors were mixed until a clear solution was obtained. Heat was then applied until the solution transitioned into a gel-like phase. The gel was then transferred to a drying oven until fully dry. Dried LFP precursor material was then ground, mixed with dried HA, and ground again to encourage thorough mixing. Samples then underwent thermal treatment in an inert atmosphere to form LFP/G. LFP reference samples using dextrose as a carbon source in place of HA were prepared following the same procedure. Samples prepared using this synthesis this method were labeled as “LFP/G A” and “LFP reference sample”.

LFP/G was also prepared by the procedure developed by Clean Republic, LLC, and the University of North Dakota. LFP precursors were mixed with HA and thermally treated to form LFP/G. Detailed information regarding the LFP/G synthesis procedure is withheld to preserve the intellectual property of Clean Republic, LLC, and the University of North Dakota. Samples prepared in this manner were labeled as “LFP/G B”.

5.2.2 Materials Characterization

Crystal purity of LFP samples was measured by X-ray diffraction (XRD) using a Rigaku Smartlab. Particle morphology was observed using a FEI Quanta 650 Field Emission Scanning Electron Microscope (SEM). Carbon contents of LFP samples were measured using a Shimadzu TOC-V Total Organic Carbon Analyzer with a SSM-5000A Solid Sample Module. A Horiba Jobin Yvon ARAMIS Raman imaging system was used to confirm and quantify the presence of graphene with respect to amorphous carbon in the samples.

5.2.3 Electrochemical Testing

Half cells utilizing LFP and LFP/G cathodes were prepared for electrochemical testing. Cathodes were prepared by first mixing a slurry comprised of 80% active LFP material, 10% conductive carbon black, and 10% PVdF binder suspended in N-methylpyrrolidone. The slurry was then cast onto an aluminum current collector at a thickness of 100-140 μm . The aluminum sheets coated with slurry were then placed into a vacuum oven to dry. Cathodes were then prepared by punching disks out of the dried aluminum/slurry sheets using a precision flat disk cutter.

Prepared cathodes were used in the assembly of CR2032 coin-type half cells. The coin cells utilized an LFP cathode and a lithium chip as a counter electrode. Separator material used was Celguard 2325 battery separator material. Electrolyte used for the cells was 1 M LiPF_6 in EC/DMC 50/50 (v/v) solution (Aldrich, 746711). The coin cells were prepared in an argon atmosphere (less than 1 ppm O_2 and H_2O).

Electrochemical testing was performed on a Neware BTS-4008 Battery Analyzer. Cells were given a rest period of 12 hours after their construction before testing occurred. The first several cycles were at a charge/discharge rate of 0.2C, and subsequent cycles were at 1C. Rate performance was tested by cycling cells at rates of 0.1C, 0.2C, 0.5C, 1C, 2C and 5C.

5.3 Results and Discussion

5.3.1 Crystal Structure Analysis by XRD

XRD analysis was conducted on all samples to initially verify the purity of the LFP crystal structure. Figure 5.3.1-1 shown below displays XRD profiles of LFP/G A, LFP/G B, and LFP reference samples. The fourth profile is peaks and intensities of typical LFP exhibiting an olivine crystal structure (Pmnb space group). All three samples

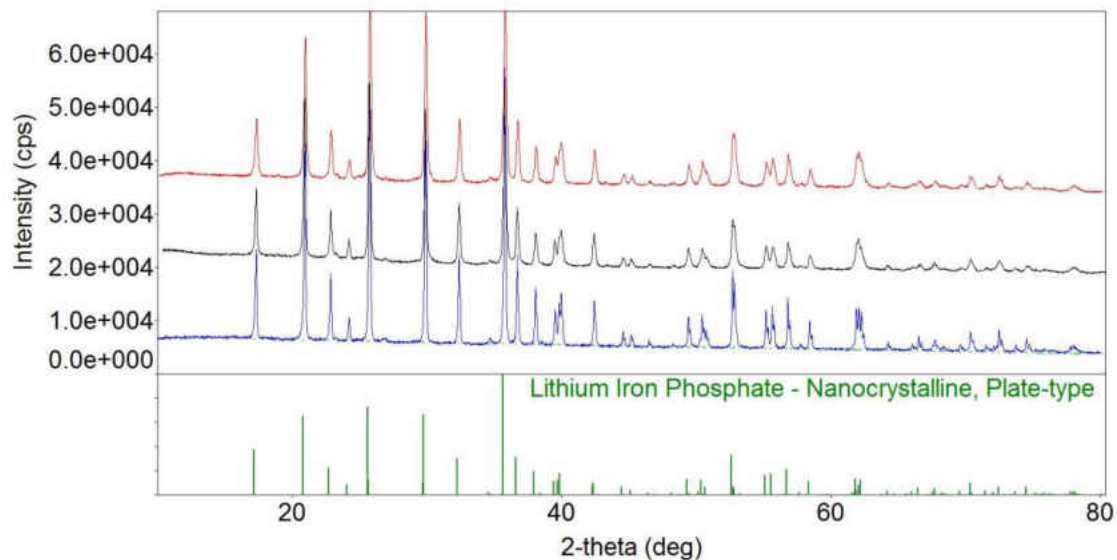


Figure 5.3.1-1 XRD Profiles of LFP/G A, LFP/G B, and LFP Reference Samples. The red top profile is the LFP reference sample, LFP/G A is the black top-middle profile, LFP/G B is blue bottom-middle, and typical olivine-structured LFP peaks and intensities are on bottom in green. Profiles are offset vertically for clarity.

exhibited excellent crystal purity, matching peak locations and intensities with the typical olivine-structured LFP. An additional peak was observed in the LFP/G A and LFP/G B samples that was not present in the LFP reference sample. This peak is located at approximately $26.5^\circ 2\theta$, and corresponds to the (002) peak of graphitized carbon. Figure 5.3.1-2 is a close-up view of this (002) graphitized carbon peak. The presence of this peak confirms that HA is forming graphitized carbon at the temperatures used for thermal treatment and LFP/G synthesis.

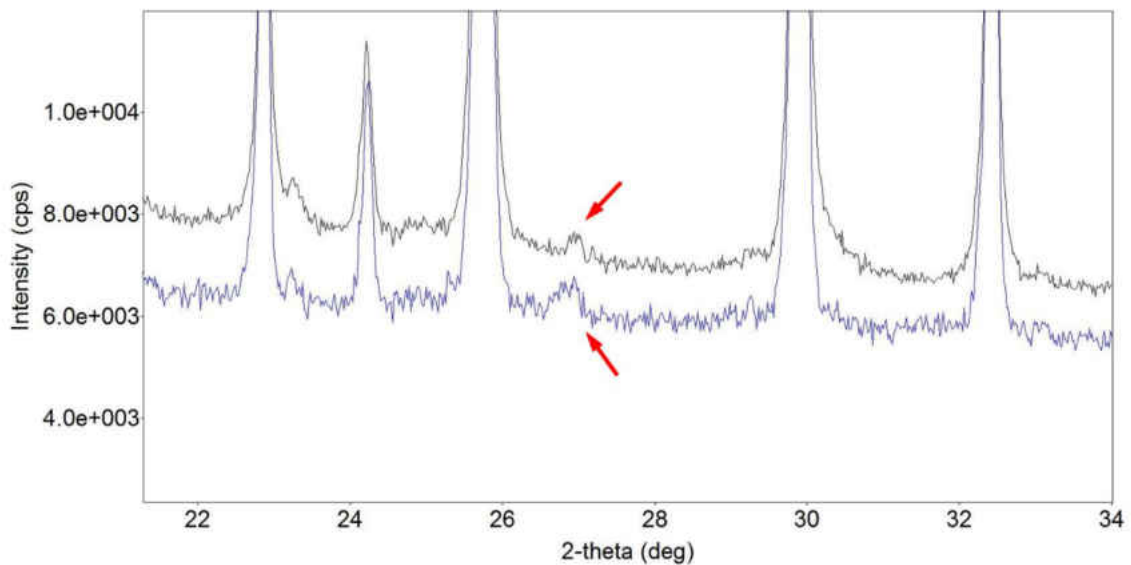


Figure 5.3.1-2 Close-up of (002) Graphitized Carbon Peak Observed in LFP/G A and LFP/G B XRD Profiles. The peaks are identified by arrows in the figure.

5.3.2 Morphology Analysis by SEM

Samples were examined using SEM to observe LFP particle size and shape, as well as products of HA that had undergone thermal treatment. Figure 5.3.2-1 shown on the following page depicts the LFP reference sample at 100x magnification.

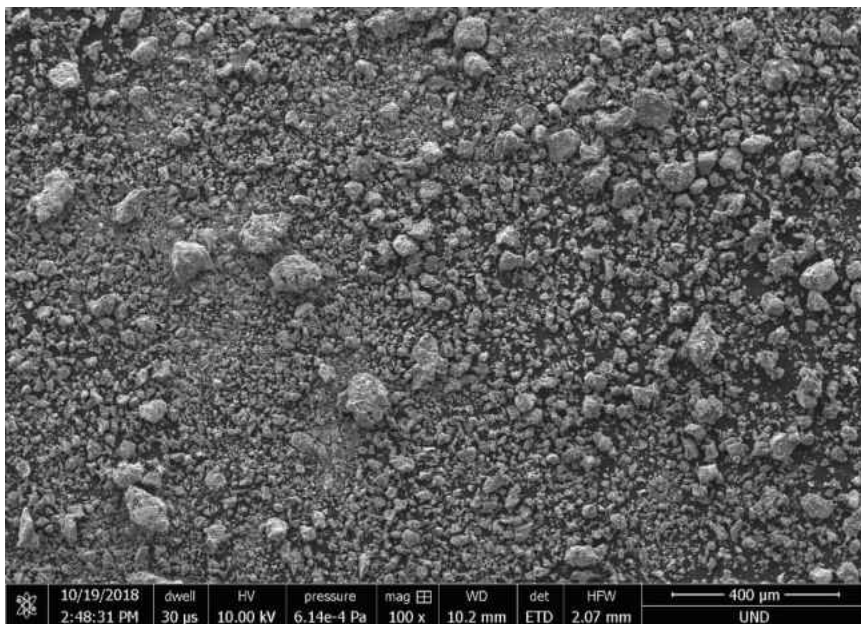


Figure 5.3.2-1 SEM Image of LFP Reference Sample at 100x Magnification.

The sample is homogeneously mixed, but there is significant variation in particle size. Closer inspection revealed angular shaped particles with nano-sized primary particles. Figure 5.3.2-2 displays the LFP reference sample at 5000x magnification. All regions

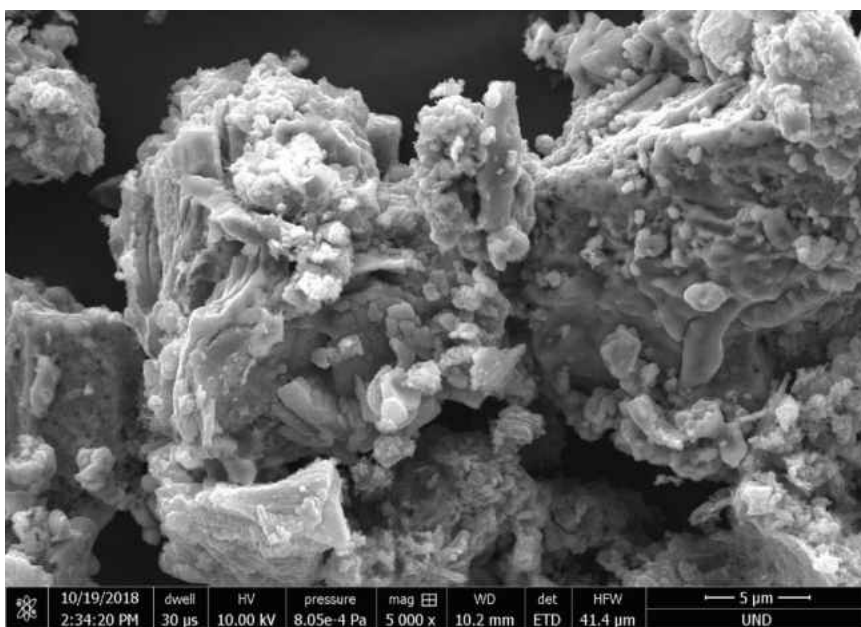


Figure 5.3.2-2 SEM Image of LFP Reference Sample at 5000x Magnification.

observed were a homogenous mixture of LFP particles and carbon, with no abnormalities.

Figure 5.3.2-3 show below is of the LFP/G A sample prepared using HA as a carbon source. It is immediately apparent that there are regions of differing composition.

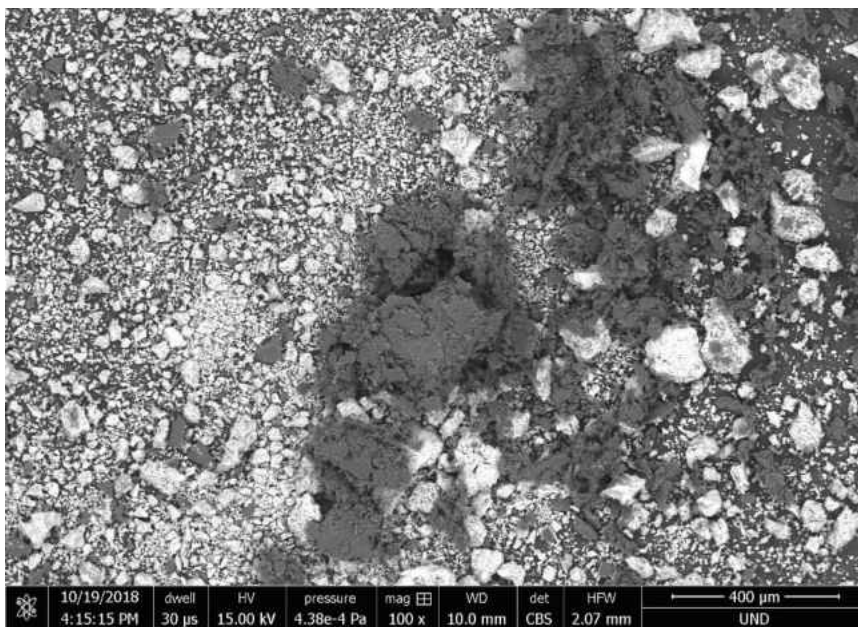


Figure 5.3.2-3 SEM Image of LFP/G A Sample at 100x Magnification.

The lighter colored particles are LFP material while the darker, flakey particles are carbon-rich, graphitized HA. Closer inspection of the boundaries these two regions revealed that although the LFP and graphitized HA particles were interacting, they were not homogeneously mixed in a manner that would facilitate enhanced electrochemical performance. Figure 5.3.2-4 depicts a region of close interaction between LFP particles and graphitized HA in the LFP/G A sample. It was also observed that the graphitized HA regions appeared to be comprised of thin sheets stacked together. At 20,000x magnification, individual particles of graphene-like carbon can be observed.

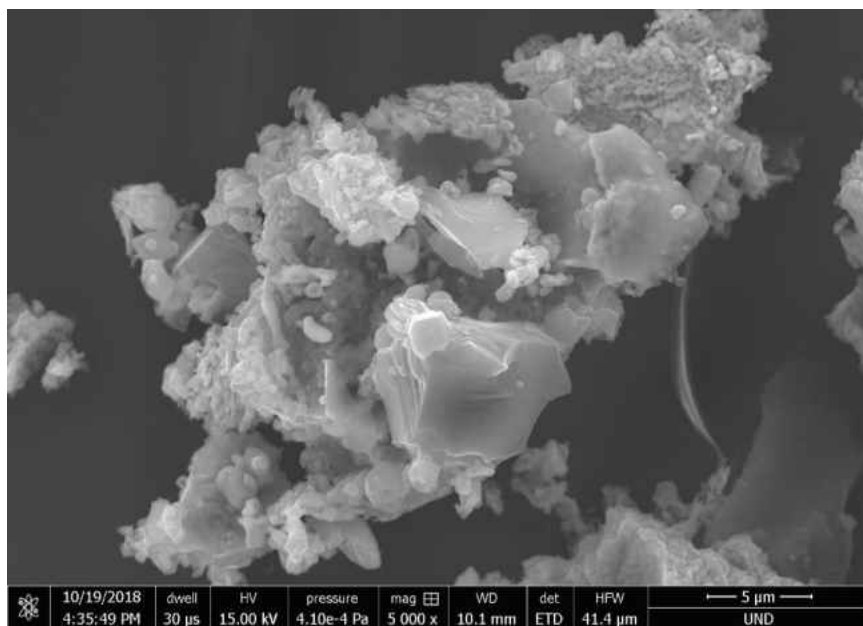


Figure 5.3.2-4 SEM Image of LFP/G A Sample at 5000x Magnification.

Figure 5.2.3-5 displays these thin carbon sheets at high magnification. These thin sheets were not observed in the reference sample which strongly indicates that they are a product of the thermal treatment of HA.

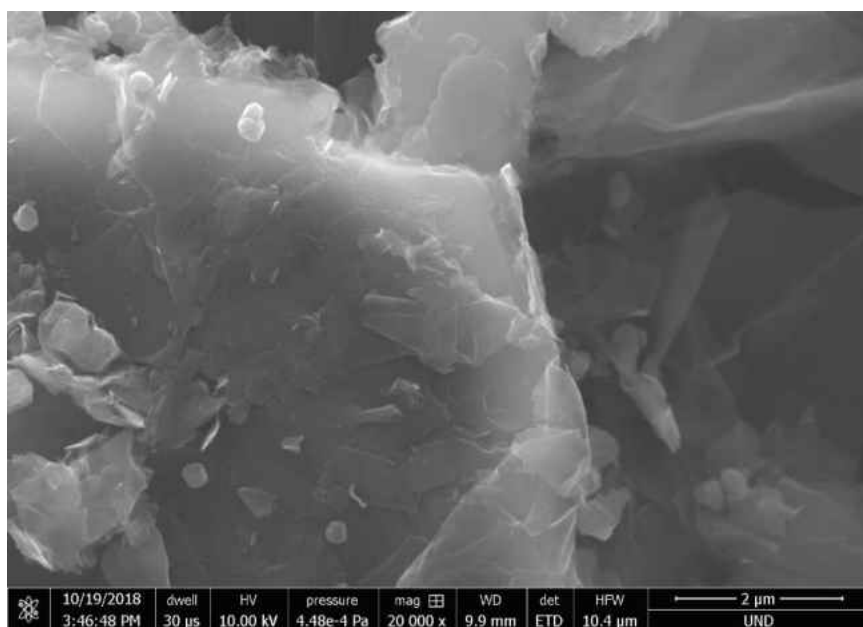


Figure 5.3.2-5 SEM Image of LFP/G A Sample at 20,000x Magnification.

Figure 5.3.2-6 displays the LFP/G B sample at 100x magnification under SEM, the sample was homogenous throughout; no hi-carbon regions were observed as in the LFP/G A sample. Due to the nature of the LFP/G B synthesis procedure, HA is able to

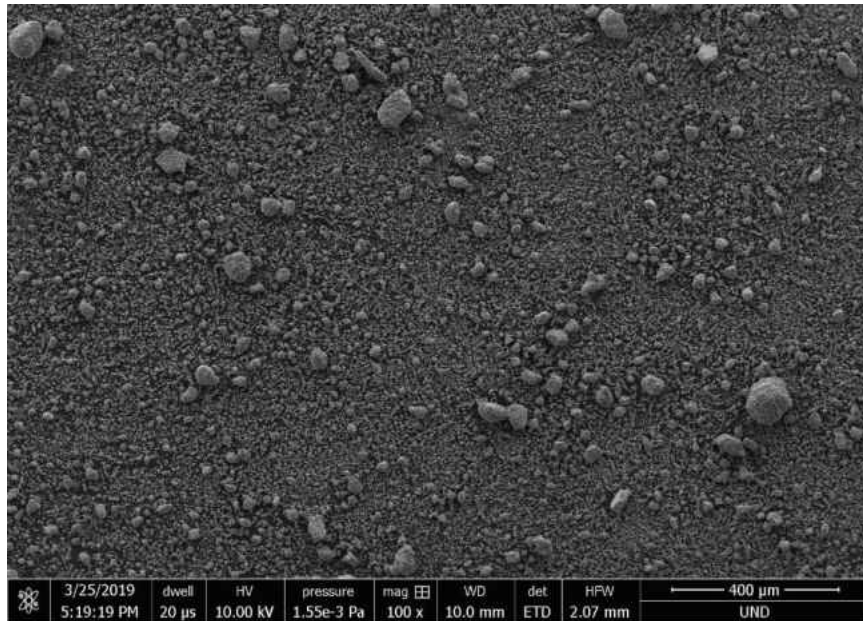


Figure 5.3.2-6 SEM Image of LFP/G B Sample at 100x Magnification.

dissolve into solution and interact with LFP precursors on a molecular level. This is likely to have resulted in a thin, even coating of graphitized carbon on the LFP particles rather than the large carbon agglomerations observed in the LFP/G A sample. Secondary LFP particles in the LFP/G B sample also did not appear to be as large as those in the LFP/G A sample. It is possible that HA is acting as a surfactant, preventing clumping and the agglomeration of LFP precursors during mixing. Closer inspection revealed nano-sized particles with rounded edges. Figure 5.3.2-7 displays the LFP/G B sample at 5,000x magnification. Particles appeared fairly uniform in size, with no obvious irregularities or anomalies.

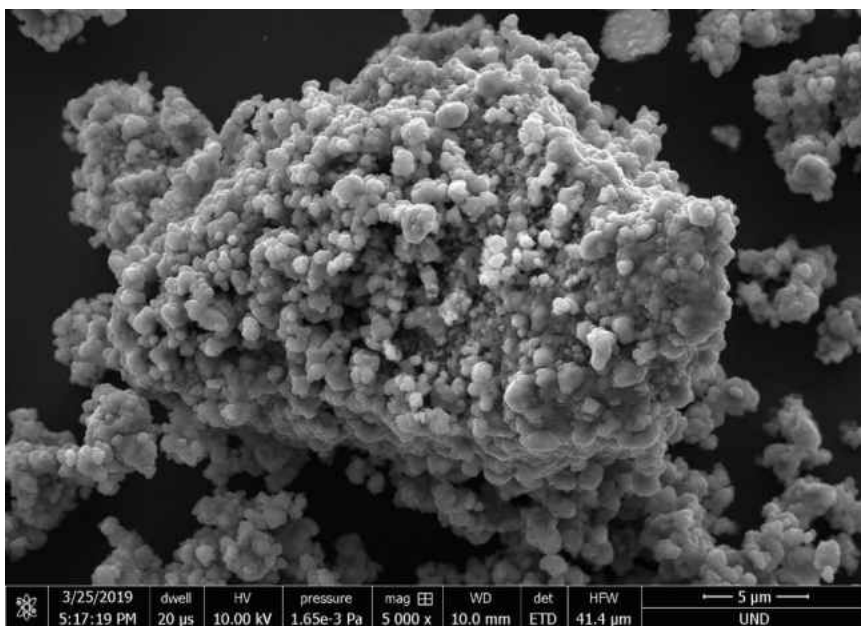


Figure 5.3.2-7 SEM Image of LFP/G B Sample at 5,000x Magnification.

5.3.3 Raman Spectrometry Analysis

Raman analysis was used to inspect samples for graphene-like carbon, and determine the ratio of ordered to amorphous carbon. Figure 5.3.3-1 compares Raman spectra for LFP/G A, LFP/G B, and LFP reference samples. The peak at 1350 cm^{-1} corresponds to the carbon D-band, representing disordered carbon, and the peak at 1580 cm^{-1} is the G-band for ordered, graphene-like carbon. The ratio of peak intensities, $I^{\text{D}}/I^{\text{G}}$, is useful metric for gauging the ratio of amorphous carbon to ordered carbon. The LFP reference sample displayed very similar intensities between the D and G peaks, having an $I^{\text{D}}/I^{\text{G}}$ ratio of 1.07. The LFP/G B sample had a G-band peak with the second highest intensity of the samples, and a $I^{\text{D}}/I^{\text{G}}$ ratio of 0.66. The LFP/G A sample the most intense G-band peak and a $I^{\text{D}}/I^{\text{G}}$ ratio of 0.53. This means that the LFP/G samples had a much higher degree of ordered carbon as a result of using HA as the carbon source.

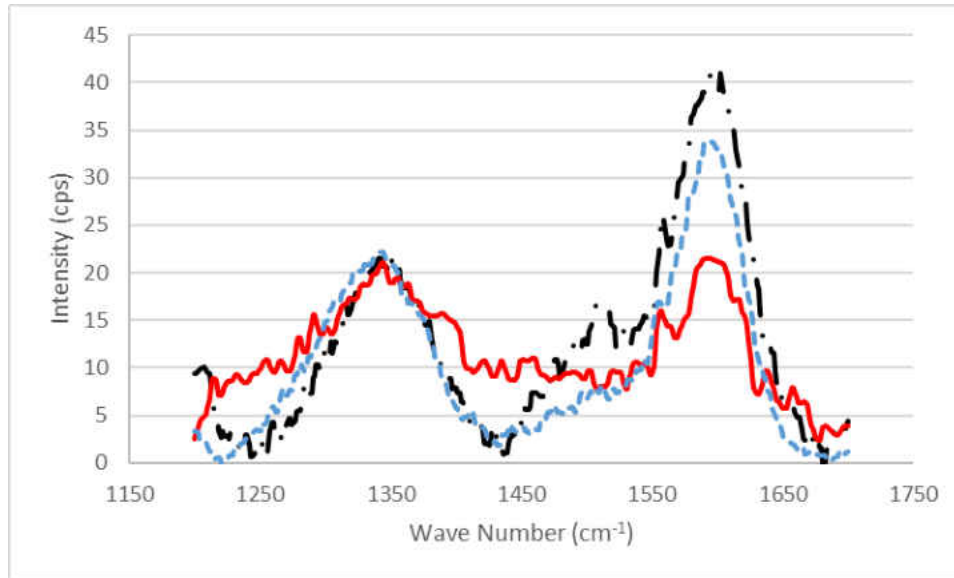


Figure 5.3.3-1 Raman Spectra of LFP/G and LFP Reference Samples. LFP reference profile is solid red line, LFP/G A profile is black dashed and dotted line, and LFP/G B profile is blue dashed line.

5.3.4 Carbon Content

Carbon contents of the LFP/G and LFP reference samples are listed below in Table 5.3.4-1. Both the LFP/G A and LFP reference samples had carbon contents which

Table 5.3.4-1 Carbon Contents for LFP/G and Reference Samples. Values are in mass percent.

Sample	Carbon Content
LFP Reference Sample	6.91%
LFP/G A	10.49%
LFP/G B	4.40%

are higher than necessary. Typical carbon contents in industrial LFP material range from about 2-6% [1]. Too much carbon can reduce the density of the active material which translates to a low specific capacity, whereas too little carbon results in low conductivity and poor cell performance. The LFP/G B sample had a more suitable carbon content for enhanced electrochemical performance.

5.3.5 Electrochemical Performance

Charge and discharge profiles at a 0.1C charge/discharge rate for coin cells prepared with LFP/G and LFP reference samples are displayed below in Figure 5.3.5-1.

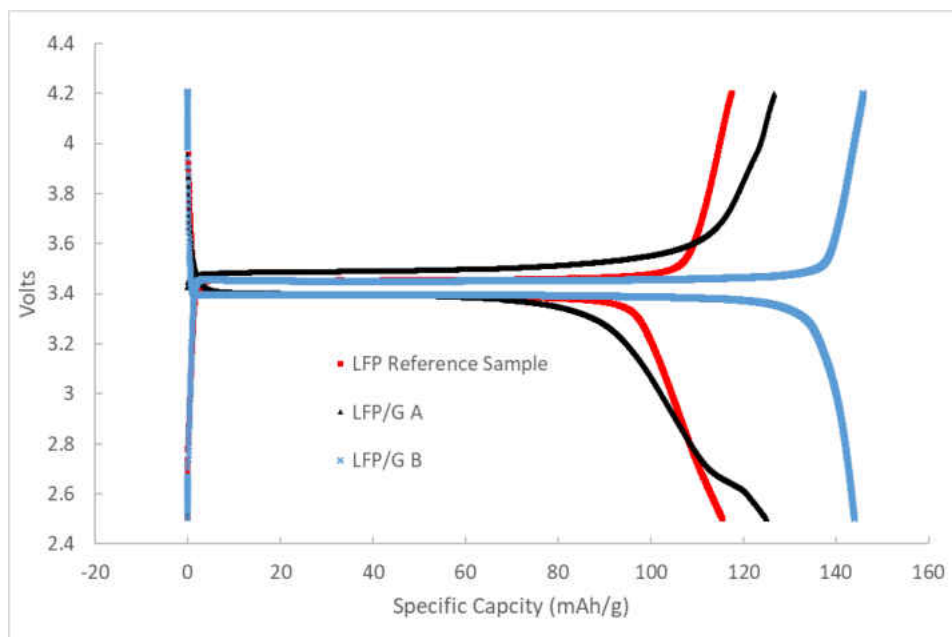


Figure 5.3.5-1 Charge/Discharge vs Voltage Profiles for Coin Cells Prepared with LFP/G and LFP Reference Samples. Data obtained while cells performed at a 0.1C charge/discharge rate.

Charging profiles begin at a capacity of zero and approximately 2.5 volts and increase with voltage. Discharge profiles begin at a capacity of zero around 4.2 volts and capacity increases as voltage drops. Specific capacity of the samples can be estimated by reading the final capacity of the discharge curve at the lower voltage cut-off point of 2.5 volts.

The specific capacity of the LFP reference sample was approximately 118 mAh/g and the LFP/G A sample was about 125 mAh/g. The LFP/G B sample had an elevated specific capacity of roughly 145 mAh/g. This increase in capacity is likely due to the synthesis procedure which allows for molecular level mixing and better LFP-HA interaction, as well as a reduced carbon content. The LFP/G A sample exhibits a distortion around 2.7V

which was not observed in the reference sample. This distortion is consistent with the anodic behavior of the insertion and de-insertion of lithium ions into layered graphene [29, 53]. A possible explanation as to why this distortion is not seen in the LFP/G B sample is because the HA was mixed with LFP particles much more homogeneously than in the LFP/G A sample. To reinforce this claim, the flaky and carbon-dense regions of graphitized HA observed under SEM in the LFP/G A sample were not observed in the LFP/G B sample.

Cycling data for coin cells prepared with LFP/G and LFP reference samples are displayed below in Figure 5.3.5-2. Cells were initially cycled at 0.2C for several cycles,

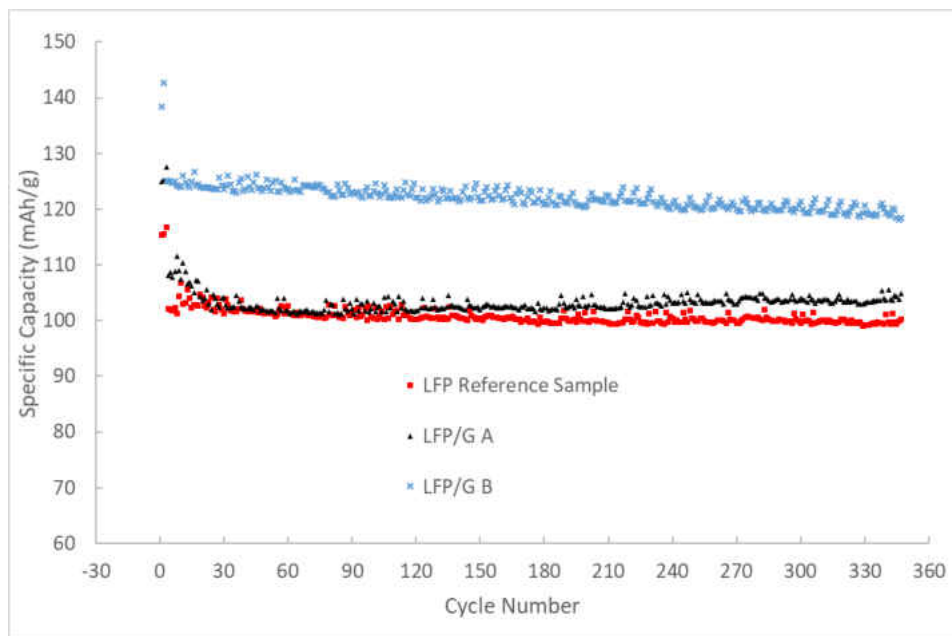


Figure 5.3.5-2 Cycling Data for Coin Cells Prepared with LFP/G and LFP Reference Samples.

and the remainder were at a charge/discharge rate of 1.0C. Vertical variation in the specific capacity of the cells was cyclical, and is likely attributed to changes in the ambient temperature of the lab that the analyzer equipment was located in. Cells prepared

with LFP/G A active material performed better than cells prepared with the reference LFP for the initial 30 cycles and then performance was approximately equal. After approximately 100 cycles, cells prepared with LFP/G A began to exhibit a slightly elevated capacity compared to that of the LFP reference material. The capacity of cells prepared with LFP/G B active material was approximately 20% higher than that of cells prepared with LFP/G A material throughout testing. This is likely due to the LFP/G B synthesis procedure and the reduced carbon content.

Rate performance testing was done by varying the charge/discharge rate of cells prepared with LFP/G and LFP reference samples. Cells were cycled at 1C, 2C, and then 5C charge/discharge rates and then returned to a rate of 1C. Figure 5.3.5-3 displays the rate performance of cells prepared with LFP/G and LFP reference active material.

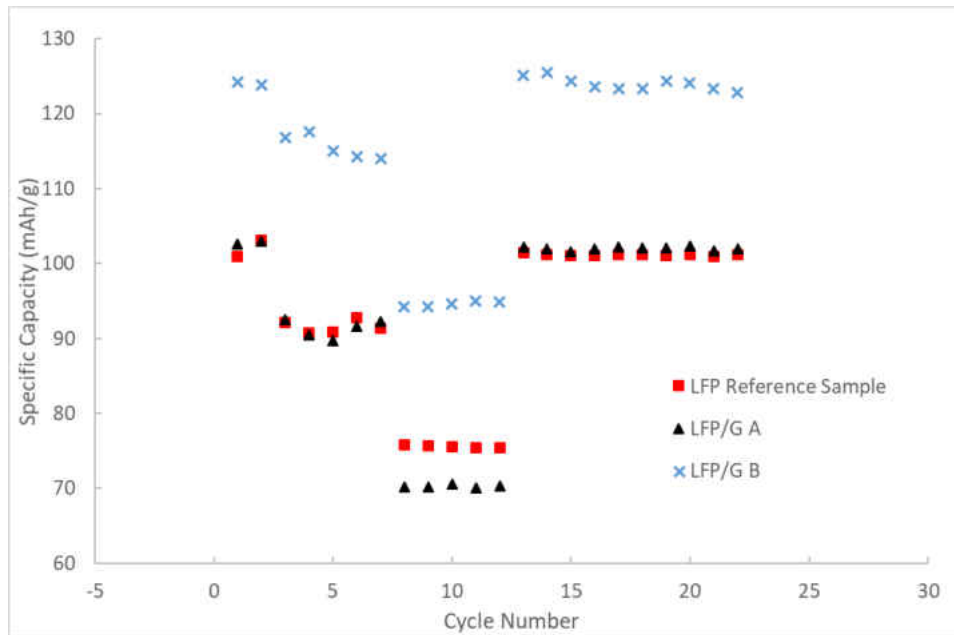


Figure 5.3.5-3 Rate Performance of Coin Cells Prepared LFP/G and LFP Reference Samples.

The LFP/G B sample displayed the highest capacity at all rates tested, retaining a capacity of almost 95 mAh/g even at a 5C charge/discharge rate. There was not a noticeable difference in performance between the LFP/G A sample and the LFP reference sample at 1C and 2C rates, and the LFP/G A sample actually performed worse than the reference sample at a 5C rate. This is theorized to be due to the high carbon content of the LFP/G A sample and the mechanism of mixing HA with LFP precursors resulting in poor LFP-HA interaction. All three samples exhibited good reversible capacity, the high charge/discharge rate of 5C had little impact on the capacity of the cells at the rate of 1C which followed rate performance testing regime.

5.4 Conclusions

XRD spectra indicated a high degree of crystal purity in both LFP/G samples as well as the reference LFP sample. Thin, graphene-like carbon plates were observed under SEM in the LFP/G A sample prepared by mixing HA with dried LFP precursor material. These plates were not found in the LFP/G B sample, and it is theorized that the superior mixing and particle interaction inherent to the LFP/G B synthesis procedure has resulted in a thin coating of graphitized HA over LFP particles rather than forming agglomerated sheets of graphene-like carbon. Raman spectra of the LFP/G samples indicated a much stronger presence of ordered, graphene-like carbon than the LFP reference material. Electrochemical testing was conducted using coin cells prepared with LFP/G and LFP reference active materials. The LFP/G A sample exhibited similar capacity, cycling ability, and rate performance to the LFP reference sample despite having a significantly higher carbon content. On capacity vs voltage plots, LFP/G A samples displayed capacity distortion around 2.7V which is consistent with the insertion and de-insertion of lithium

into graphene. LFP/G B coin cells had the highest specific capacity at 145 mAh/g at 0.1C as well as retained capacity the best during high-rate testing. This is thought to be due to better interaction between the LFP material and the graphitized HA as a result of the synthesis procedure.

These findings are all indicators that HA can successfully reduce to graphene-like carbon by the thermal treatment used to synthesize LFP active material. This graphitized HA exhibits physical, chemical, and electrochemical traits of few-layer graphene. Coin cells prepared with active material synthesized using HA have benefited from enhanced capacity and performance. These results can be used to conclude that leonardite-derived HA is suitable for highly technical applications such as a carbon source for LIB electrode materials.

6 FUTURE INSIGHTS

6.1 Continuation of Research

6.1.1 Overview

There are multiple possible research opportunities based on the outcomes of this research. Areas of interest for immediate study would include optimizing the LFP/G synthesis procedure, further investigation into possible methods for fractioning HAs, and the impact of fractioned HA on graphene formation and electrochemical performance active materials. Other potential research areas could include the preparation of both anode and cathode materials modified with HA for use in lithium or other battery types. Another possible area of study would be integrating the HA extraction and purification procedure with a process for upgrading coal, as there are some shared similarities. Because of the nature of this work and the many potential applications for graphene and graphene-like materials, it can be expected that research with HA will continue to grow in the future.

6.1.2 Optimization of Graphene-Modified Lithium Iron Phosphate Synthesis Procedure

While it was demonstrated that HA is capable of producing graphene-like carbon and enhancing the performance of LIBs, the LFP/G synthesis procedure has ample room for optimization. Various factors affecting graphene formation can be adjusted to achieve optimal results and enhanced electrochemical performance. Sintering temperature,

sintering time, preheat temperature, and mass percent of HA added are all factors which may have a significant impact on graphene formation and cell performance. The procedure can be optimized based on responses such as: specific capacity of LFP/G active material, high-rate performance of cells prepared with active material, carbon content and tap density of LFP/G, and Raman I^D/I^G ratio of the LFP/G material. Once fully optimized, the synthesis procedure should yield a LFP/G material with excellent electrochemical performance and longevity.

6.1.3 Fractionation of Humic Acid

Fractionation of humic substances is of particular interest, as different fractions may produce graphene different with different properties. Various techniques have been employed to segregate HA into various factions by methods including manipulating solution composition, pH control, solvents in which HA is selectively soluble, and by using methods based on Stokes' law [13, 16, 22, 49, 51, 54-57]. Theoretically, larger HA particles should form larger graphene sheets with fewer surface imperfections. The impact of HA fraction on the Raman I^D/I^G ratio would be of interest if any correlation was discovered. Some preliminary data was collected in parallel with this work in which HA was fractionated by controlling solution pH and by centrifuging. It was hypothesized that larger HA particles would precipitate out of solution at higher pH values, while lower-weight molecules would remain in solution. Initial results indicate that these two fractionation methods are somewhat successful at segregating HA based on molecular size.

HA segregated into fractions based on molecule size could potentially be incorporated into the LFP/G synthesis optimization research. Ideally, a method of

fractionation could be used to obtain a fraction of HA capable of forming a thin, porous graphene coating on LFP particles or other desired substrate. This should increase the electrochemical performance of LFP/G materials prepared with the fractioned HA.

6.2 Potential Applications

While graphene use is becoming more and more popular due to the exceptional characteristics of the material, graphene precursors still remain rather expensive. A popular method of producing graphene materials is through the reduction of GO, which can be quite expensive. Conversely, the work here has demonstrated that HA can be utilized as a low cost replacement for expensive graphene precursors. HA could potentially be used as a direct replacement for GO for applications such as composites embedded with graphene particles, graphene-based nano-filters, and in uses requiring conductive coatings for optical applications such as touchscreens [30]. As this research has demonstrated, HA should be considered a viable graphene precursor material suitable for a variety of technical applications.

Potential applications utilizing HA for uses other than graphene preparation also exist. Humic materials demonstrate a strong ability to bind with metal ions and form robust HA-metal complexes. Because of this, HA could be utilized as a sort of ion-exchange material allowing for targeted metal recovery from sources such as brines. This trait could be exploited for applications such as upgrading coal by removing humic materials which are bound to metals and ash. Residual material left over from HA extraction could also be utilized to prepare other highly-technical carbon-based products. While extracting high-purity HA was the focus of this study, there are multiple applications where this process could be applied to fulfil a variety of objectives.

REFERENCES

- [1] J. Wang and X. Sun, "Understanding and recent development of carbon coating on LiFePO₄ cathode materials for lithium-ion batteries," *Energy & Environmental Science*, vol. 5, pp. 5163-5185, Jan 1, 2012.
- [2] D. Jugović and D. Uskoković, "A review of recent developments in the synthesis procedures of lithium iron phosphate powders," *Journal of Power Sources*, vol. 190, pp. 538-544, 2009.
- [3] E.M. Duraia, S. Niu, G.W. Beall and C.P. Rhodes, "Humic acid-derived graphene–SnO₂ nanocomposites for high capacity lithium-ion battery anodes," *Journal of Materials Science: Materials in Electronics*, vol. 29, pp. 8456-8464, May. 2018.
- [4] X. Zhou, F. Wang, Y. Zhu and Z. Liu, "Graphene modified LiFePO₄ cathode materials for high power lithium ion batteries," *Journal of Materials Chemistry*, vol. 21, pp. 3353, 2011.
- [5] R. Mo, Z. Lei, D. Rooney and K. Sun, "Facile synthesis of nanocrystalline LiFePO₄/graphene composite as cathode material for high power lithium ion batteries," *Electrochimica Acta*, vol. 130, pp. 594-599, Jun 1, 2014.
- [6] G.W. Beall, "Method and System for Producing Graphene and Functionalized Graphene," Jun 6, 2013.
- [7] H.R. Schulten and M. Schnitzer, "A state of the art structural concept for humic substances," *The Science of Nature*, vol. 80, pp. 29-30, 1993.
- [8] L. Leonardite Products, "Source Leonardite Properties," vol. 2019, Ap. 2017.
- [9] C. Sprengel, "Über pflanzenhumus, humussaure und humussaure salze," *Kastner's Arch. Ges. Naturlehre*, vol. 8, pp. 145, 1826.
- [10] C.M. Frost, J.J. Hoeppe and W.W. Fowkes, "Source and General Properties of Humic Acids from Lignitic Materials," *Journal of Chemical & Engineering Data*, vol. 4, pp. 173-176, Apr. 1959.
- [11] International Humic Substances Society, "Outline of extraction procedures," 1981.
- [12] S. Kuwatsuka, A. Watanabe, K. Itoh and S. Arai, "Comparison of two methods of preparation of humic and fulvic acids, IHSS method and NAGOYA method," *Soil Science and Plant Nutrition*, vol. 38, pp. 23-30, Mar. 1992.

- [13] G. Thiessen and C.J. Engelder, "Isolation of the Humic Acids," *Industrial & Engineering Chemistry*, vol. 22, pp. 1131-1133, Oct. 1930.
- [14] T.S. Polansky and C.R. Kinney, "Solvent Extraction of Humic Acids from Nitric Acid-Treated Bituminous Coal," *Industrial & Engineering Chemistry*, vol. 39, pp. 925-929, Jul. 1947.
- [15] R.W. Youngs and C.M. Frost, "Humic acids from Leonardite: a soil conditioner and organic fertilizer," pp. 12-17, Jan 1, 1963.
- [16] M.H.B. Hayes, R.S. Swift, R.E. Wardle and J.K. Brown, "Humic materials from an organic soil: A comparison of extractants and of properties of extracts," *Geoderma*, vol. 13, pp. 231-245, 1975.
- [17] A. Piccolo, "Characteristics of Soil Humic Extracts Obtained by Some Organic and Inorganic Solvents and Purified by HCl-HF Treatment," *Soil Science*, vol. 146, pp. 418-426, Dec. 1988.
- [18] G. Ricca, F. Severini, G. Di Silvestro, C.M. Yuan and F. Adani, "Derivatization and structural studies by spectroscopic methods of humic acids from Leonardite," *Geoderma*, vol. 98, pp. 115-125, 2000.
- [19] L.D. Friedman and C.R. Kinney, "Humic Acids from Coal. Controlled Air-Oxidation of Coals and Carbons at 150° to 400° C," *Industrial & Engineering Chemistry*, vol. 42, pp. 2525-2529, Dec. 1950.
- [20] G.W. Beall, E.M. Duraia, Q. Yu and Z. Liu, "Single crystalline graphene synthesized by thermal annealing of humic acid over copper foils," *Physica E: Low-Dimensional Systems and Nanostructures*, vol. 56, pp. 331-336, Feb. 2014.
- [21] E.M. Duraia, B. Henderson and G.W. Beall, "Reduced humic acid nanosheets and its uses as nanofiller," *Journal of Physics and Chemistry of Solids*, vol. 85, pp. 86-90, Oct. 2015.
- [22] F.J. Stevenson, "Extraction, Fractionation, and General Chemical Composition of Soil Organic Matter," in *Humus chemistry : genesis, composition, reactions*, New York: Wiley, 1982, pp. 26-54.
- [23] J.M. Garcia-Mina, "Stability, solubility and maximum metal binding capacity in metal-humic complexes involving humic substances extracted from peat and organic compost," *Organic Geochemistry*, vol. 37, pp. 1960-1972, 2006.
- [24] S. Hori and A. Okuda, "Purification of humic acid by the use of ion exchange resin," *Soil Science and Plant Nutrition*, vol. 7, pp. 4, Jul. 1961.

- [25] D.L. Sparks, *Methods of soil analysis. Part 3, Chemical methods*, Madison, Wisconsin USA: Soil Science Society of America, Inc., 1996, .
- [26] H.A. Flaschka, *EDTA Titrations: an Introduction to Theory and Practice*, New York [u.a.]: Pergamon Press, 1959, .
- [27] Y. Li and N. Chopra, "Progress in Large-Scale Production of Graphene. Part 1: Chemical Methods," *Jom*, vol. 67, pp. 34-43, Jan. 2015.
- [28] Z. Qiao, M. Chen, C. Wang and Y. Yuan, "Humic acids-based hierarchical porous carbons as high-rate performance electrodes for symmetric supercapacitors," *Bioresource Technology*, vol. 163, pp. 386-389, Jul. 2014.
- [29] B. Xing, H. Zeng, G. Huang, C. Zhang, R. Yuan, Y. Cao, Z. Chen and J. Yu, "Porous graphene prepared from anthracite as high performance anode materials for lithium-ion battery applications," *Journal of Alloys and Compounds*, vol. 779, pp. 202-211, Mar 30, 2019.
- [30] C. Powell and G.W. Beall, "Graphene oxide and graphene from low grade coal: Synthesis, characterization and applications," *Current Opinion in Colloid & Interface Science*, vol. 20, pp. 362-366, Oct. 2015.
- [31] S. Baskakov, A. Lobach, S. Vasil'ev, N. Dremova, V. Martynenko, A. Arbuzov, Y. Baskakova, A. Volodin, V. Volkov, V. Kazakov and Y. Shul'ga, "High-temperature carbonization of humic acids and a composite of humic acids with graphene oxide," *High Energy Chem*, vol. 50, pp. 43-50, Jan. 2016.
- [32] E.M. Duraia and G.W. Beall, "Large temperature-induced red shift of G-band of functionalized graphene nanosheets synthesized from humic acid," *Superlattices and Microstructures*, vol. 98, pp. 379-384, Oct. 2016.
- [33] D. SI, G. Huang, C. Zhang, B. Xing, Z. Chen, L. Chen and H. Zhang, "Preparation and Electrochemical Performance of Humic Acid-based Graphitized Materials," *Materials Guide A: Overview*, vol. 32, pp. 368-372, Feb. 2018.
- [34] L. Yuan, Z. Wang, W. Zhang, X. Hu, J. Chen, Y. Huang and J.B. Goodenough, "Development and challenges of LiFePO₄ cathode material for lithium-ion batteries," *Energy & Environmental Science*, vol. 4, pp. 269, 2011.
- [35] J. Zhu, R. Duan, S. Zhang, N. Jiang, Y. Zhang and J. Zhu, "The application of graphene in lithium ion battery electrode materials," *SpringerPlus*, vol. 3, pp. 1-8, Dec. 2014.

- [36] Haixia Wu Qinjiao Liu Shouwu Guo, "Composites of Graphene and LiFePO₄ as Cathode Materials for Lithium-Ion Battery: A Mini-review," *Nano-Micro Lett*, vol. 6, pp. 316-326, 2014.
- [37] J. Yang, D. Wang, J. Wang, R. Li, X. Li, D. Geng, G. Liang, M. Gauthier and X. Sun, "3D porous LiFePO₄/graphene hybrid cathodes with enhanced performance for Li-ion batteries," *Journal of Power Sources*, vol. 208, pp. 340-344, Jun 15, 2012.
- [38] Y. Zhang, W. Wang, P. Li, Y. Fu and X. Ma, "A simple solvothermal route to synthesize graphene-modified LiFePO₄ cathode for high power lithium ion batteries," *Journal of Power Sources*, vol. 210, pp. 47-53, Jul 15, 2012.
- [39] K.S. Dhindsa, B.P. Mandal, K. Bazzi, M.W. Lin, M. Nazri, G.A. Nazri, V.M. Naik, R. Naik, V.K. Garg, A.C. Oliveira, P. Vaishnava and Z.X. Zhou, "Enhanced electrochemical performance of graphene modified LiFePO₄ cathode material for lithium ion batteries," *Solid State Ionics*, vol. 253, pp. 94-100, Dec 15, 2013.
- [40] H. Liu, C. Miao, Y. Meng, Q. Xu, X. Zhang and Z. Tang, "Effect of graphene nanosheets content on the morphology and electrochemical performance of LiFePO₄ particles in lithium ion batteries," *Electrochimica Acta*, vol. 135, pp. 311-318, Jul 20, 2014.
- [41] S. Tao, W. Huang, Z. Wu, G. Wu, X. Zhu, S. Wang, X. Wang, M. Zhang, W. Chu and L. Song, "Performance enhancement of Lithium-ion battery with LiFePO₄@C/RGO hybrid electrode," *Electrochimica Acta*, vol. 144, pp. 406-411, Oct 20, 2014.
- [42] C. Su, X. Bu, L. Xu, J. Liu and C. Zhang, "A novel LiFePO₄/graphene/carbon composite as a performance-improved cathode material for lithium-ion batteries," *Electrochimica Acta*, vol. 64, pp. 190-195, Mar 1, 2012.
- [43] L. Wen, J. Sun, L. An, X. Wang, X. Ren and G. Liang, "Effect of Conductive Material Morphology on Spherical Lithium Iron Phosphate," *Nanomaterials (Basel, Switzerland)*, vol. 8, pp. 904, Nov 5, 2018.
- [44] Y. Huang, H. Liu, Y. Lu, Y. Hou and Q. Li, "Electrophoretic lithium iron phosphate/reduced graphene oxide composite for lithium ion battery cathode application," *Journal of Power Sources*, vol. 284, pp. 236-244, Jun 15, 2015.
- [45] W. Shen, Y. Wang, J. Yan, H. Wu and S. Guo, "Enhanced Electrochemical Performance of Lithium Iron(II) Phosphate Modified Cooperatively via Chemically Reduced Graphene Oxide and Polyaniline," *Electrochimica Acta*, vol. 173, pp. 310-315, Aug. 2015.

- [46] S. Feng, W. Shen and S. Guo, "Effects of polypyrrole and chemically reduced graphene oxide on electrochemical properties of lithium iron (II) phosphate," *J Solid State Electrochem*, vol. 21, pp. 3021-3028, Oct. 2017.
- [47] Y. Zhang, Y. Huang, X. Wang, Y. Guo, D. Jia and X. Tang, "Improved electrochemical performance of lithium iron phosphate in situ coated with hierarchical porous nitrogen-doped graphene-like membrane," *Journal of Power Sources*, vol. 305, pp. 122-127, Feb 15, 2016.
- [48] Y. Wang, Y. Wang, Z. He, C. Fan, C. Liu, Q. Peng, J. Chen and Z. Feng, "Preparation and characterization of flexible lithium iron phosphate/graphene/cellulose electrode for lithium ion batteries," *Journal of Colloid and Interface Science*, vol. 512, pp. 398-403, Feb 15, 2018.
- [49] H. Kipton, J. Powell and R.M. Town, "Solubility and fractionation of humic acid; effect of pH and ionic medium," *Analytica Chimica Acta*, vol. 267, pp. 47-54, 1992.
- [50] J. Kandráč, M. Hutta and M. Foltin, "Preparation and characterization of humic and fulvic acid working standards—practical experience," *Journal of Radioanalytical and Nuclear Chemistry Articles*, vol. 208, pp. 577-592, Sep. 1996.
- [51] I. Christl, H. Knicker, I. Kögel-Knabner and R. Kretzschmar, "Chemical heterogeneity of humic substances: characterization of size fractions obtained by hollow-fibre ultrafiltration," *European Journal of Soil Science*, vol. 51, pp. 617-625, Dec. 2000.
- [52] W.E. Kline and H.S. Fogler, "Dissolution of silicate minerals by hydrofluoric acid," *Industrial & Engineering Chemistry Fundamentals*, vol. 20, pp. 155-161, May. 1981.
- [53] J. Hassoun, F. Bonaccorso, M. Agostini, M. Angelucci, M.G. Betti, R. Cingolani, M. Gemmi, C. Mariani, S. Panero, V. Pellegrini and B. Scrosati, "An Advanced Lithium-Ion Battery Based on a Graphene Anode and a Lithium Iron Phosphate Cathode," *Nano Letters*, vol. 14, pp. 4901-4906, Aug 13, 2014.
- [54] V.A. Beckley, "The preparation and fractionation of humic acid," *The Journal of Agricultural Science*, vol. 11, pp. 66-68, Jan 1, 1921.
- [55] K. Kumada and Y. Kawamura, "On the fractionation of humic acids by a fractional precipitation technique," *Soil Science and Plant Nutrition*, vol. 14, pp. 198-200, Sep. 1968.
- [56] B. Lee, Y. Seo and J. Hur, "Investigation of adsorptive fractionation of humic acid on graphene oxide using fluorescence EEM-PARAFAC," *Water Research*, vol. 73, pp. 242-251, Apr 15, 2015.

- [57] S. Qian, W. Ding, Y. Li, G. Liu, J. Sun and Q. Ding, "Characterization of humic acids derived from Leonardite using a solid-state NMR spectroscopy and effects of humic acids on growth and nutrient uptake of snap bean," *Chemical Speciation & Bioavailability*, vol. 27, pp. 156-161, Oct 2, 2015.